AFOSR TN 60-1386

THE JOHNS HOPKINS UNIVERSITY

DEPARTMENT OF MECHANICS

THE AERODYNAMICS OF MASS LOSS AND MASS GAIN OF STARS

by

Francis H. Clauser

November 1960

Baltimore 18, Maryland

AFOSR TN 60-1386

THE AERODYNAMICS OF MASS LOSS AND MASS GAIN OF STARS

by

Francis H. Clauser
The Johns Hopkins University

November 1960

This research was supported by the United States Air Force through the Air Force Office of Scientific Research of the Air Research and Development Command, under Contract Number AF 49(638)-496. Reproduction in whole or in part is permitted for any purpose of the United States Government.

The Aerodynamics of Mass Loss and Mass Gain of Stars

Francis H. Clauser
The Johns Hopkins University

Foreward

The present paper was written as a result of the discussions at the Cosmical Gas Dynamics Symposium which took place in Varenna, Italy in August 1960. Although the writing of the present paper was undertaken by F. H. Clauser, the paper itself contains many results that were obtained by Armand Deutsch, Paul Germain, Eugene Parker and other members of the conference. If it would have been possible to credit these men with authorship without imposing upon them responsibilities for shortcomings that may appear in the present paper, this would have been done.

Introduction

A star, being a hot object, tends to boil away its mass into interstellar space. The gravitational field of the star acts to check such a mass loss. If the boiling is considered as taking place at the surface of the star and if the atmosphere of the star obeys a polytropic law with any reasonable exponent, then for almost all stars, the combination of stellar mass, radius and surface temperature is such that the gravitational field can effectively hold the atmosphere to the star. This can be perhaps most readily understood in the following way. The equilibrium equations for an atmosphere show that for this atmosphere to escape, the thermal velocities of the gas at the surface must exceed some multiple of the escape velocity at the surface of the star (the exact value of the multiple depends upon the polytropic exponent and is not far from unity for "reasonable" exponents). Since stellar surface temperatures correspond, in most cases, to particle velocities far less than the escape speed, the truth of the above assertation is apparent.

However, we know that in the corona of a star, the atmosphere does not follow a polytropic law with any "reasonable" exponent. Instead, the temperature rises relatively abruptly to values of the order 10^{6}°K. If we regard the corona as being an extraordinary region, and suppose that the atmosphere starts at the outer limits of the corona, and obeys a polytropic law outward, then the picture is quite different. With outer coronal surface temperatures of the order of millions of degrees, the thermal speeds become comparable with the escape velocities at the outer coronal surface and the gravitational field is no longer an assured barrier against the boiling away of the stellar atmosphere.

However, the gravitational field is not the only agent acting to prevent a steady ebullition of the mass of stars. The interstellar reservoir is not empty, but contains a gas whose pressure, aided by the gravitational fields of the stars, attempts to force a flow of matter back into the stars.

Because of the great diversity of stars, it is unlikely that a nice balance of these factors exists for all stars: consequently we should not expect stellar atmospheres to be in static equilibrium with no inflow or outflow. Rather we should expect that a flow will be an essential part of the dynamic equilibrium of stellar atmospheres.

An Illustrative Example of Aerodynamic Flow

Aerodynamic experience shows that even simple flows of compressible flows, being nonlinear processes, lead to puzzling dilemmas if one expects, on the basis of experience with linear phenomena, to obtain unique, continuous solutions to the differential equations describing the flows. To illustrate this state of affairs, and to lay the groundwork for problems that will confront us later, let us consider the example shows in figure 1. The liquid in the lower container is maintained at a fixed level and a fixed temperature. The area of the surface of this liquid is A_L. This lower container is connected by a constricted pipe of throat area, A_T, to a large reservoir in which the pressure p_R may be set at any level by means

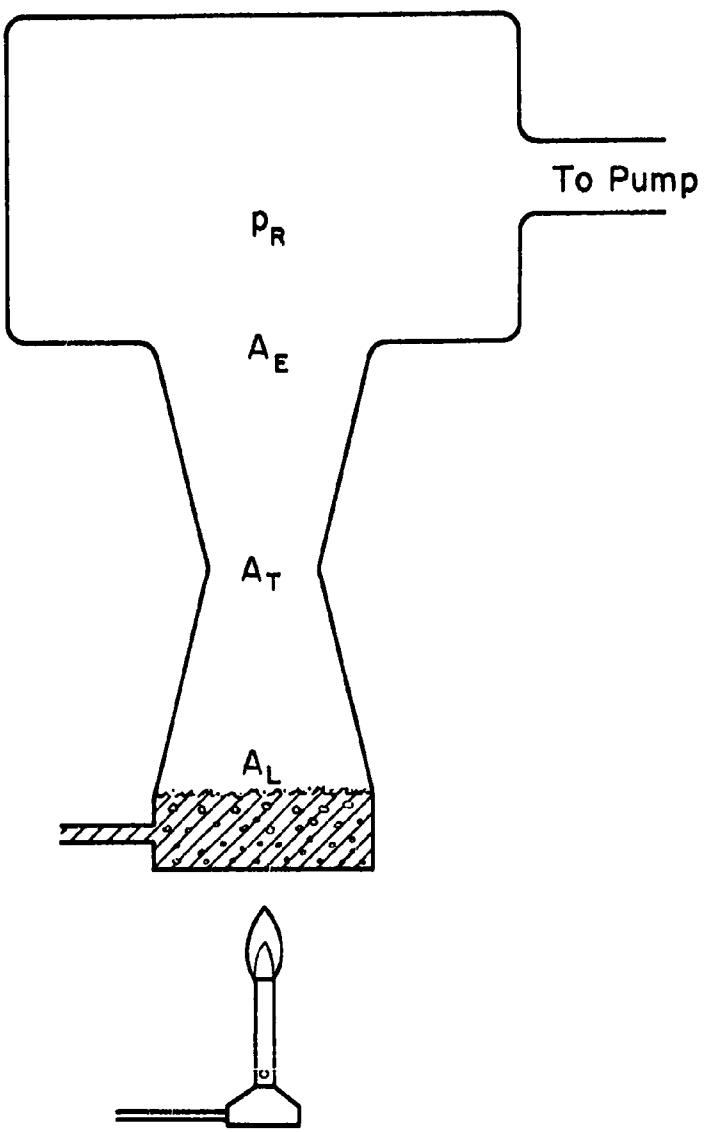

Figure 1

of a pump. The area of the pipe at the section which empties into the reservoir is A .

We are now interested in the whole range of equilibrium flows that will occur for the various levels of pressure which can be set in the upper reservoir. Clearly, when the reservoir pressure equals the vapor pressure of the liquid, no flow will occur. For greater or lesser reservoir pressures there will be a flow to or from the lower container, with evaporation or condensation taking place at the liquid surface. What determines the magnitude of these flows and what functional relationship will they bear to the pressure in the reservoir?

To answer this question without undue complexity, we assume the flow to be frictionless and to be substantially uniform across each section of the pipe connecting the lower container to the upper reservoir. We also assume that the isentropic law for the gas can be represented in the form $p = \kappa\rho^{\gamma}$, where p is the pressure, ρ the density and γ is the ratio of the specific heats. The Bernoulli equation for the gas can then be written $\frac{u^2}{2} + \frac{c^2}{\gamma-1} = B$ where B is the Bernoulli constant, u is the velocity of the gas, and c is the local velocity of sound. If A is the local cross-sectional area of the pipe, then $\rho uA = \phi$ where ϕ is a constant representing the mass flow in the pipe. The velocity of sound is related to the pressure, density and temperature by the following relations:
$c^2 = \gamma RT = \gamma p/\rho$.

In the above problem, the natural independent variable would appear to be the distance along the pipe, with the area of the pipe being expressed in terms of this variable. However, it is an interesting fact that this distance variable does not enter directly into the equation for the gas flow. As a consequence, it is appropriate to take the pipe area itself as the independent variable. If we express the velocity, the density and the pressure all as functions of this area, we have

$$\frac{u^2}{2} + \frac{\gamma\kappa}{\gamma-1}\left(\frac{\phi}{uA}\right)^{\gamma-1} = B$$

$$\frac{1}{2}\left(\frac{\phi}{\rho A}\right)^2 + \frac{\gamma\kappa}{\gamma-1}\rho^{\gamma-1} = B$$

$$\frac{1}{2}\left(\frac{\phi}{A}\right)^2\left(\frac{\kappa}{p}\right)^{2/\gamma} + \frac{\gamma}{\gamma-1}\kappa^{1/\gamma}p^{\frac{\gamma-1}{\gamma}} = B$$

We see that these relationships between u, ρ, and p on the one hand and A on the other involve the four constants B, γ, κ and ϕ. Since our desire is to explore the full range of behavior of such flows, we see that if we proceed blindly, plotting u, p and ρ versus A for all possible values of B, γ, κ and ϕ, we are faced with an enormous amount of work. However, it is possible to avoid this distasteful prospect. In spite of all the diverse ways in which the constants B, γ, κ and ϕ enter the above equations, their effect on the behavior of the flow is relatively simple. They can, in fact, be largely absorbed by changing the scales used to plot the results. We can simplify the algebra of such scale changes by introducing the critical velocity, $u_* = \sqrt{2\frac{\gamma-1}{\gamma+1}B}$ which is the flow velocity at Mach one, i.e. u = c. Correspondingly we have

$$\rho_* = \left(\frac{u_*^2}{\gamma\kappa}\right)^{\frac{1}{\gamma-1}} \quad , \quad p_* = \kappa\rho_*^{\gamma} \quad \text{and} \quad A_* = \frac{\phi}{\rho_* u_*} .$$

If we now use these constants as scale factors for the corresponding variables, we have:

$$\frac{\gamma-1}{2}\left(\frac{u}{u_*}\right)^2 + \frac{1}{\left(\frac{u}{u_*}\cdot\frac{A}{A_*}\right)^{\gamma-1}} = \frac{\gamma+1}{2}$$

$$\frac{\gamma-1}{2}\left(\frac{\rho}{\rho_*}\frac{A}{A_*}\right)^2+\left(\frac{\rho}{\rho_*}\right)^{\gamma-1}=\frac{\gamma+1}{2}$$

$$\frac{\gamma-1}{2}\left(\frac{p}{p_*}\right)^{\frac{2}{\gamma}}\left(\frac{A}{A_*}\right)^2+\left(\frac{p}{p_*}\right)^{\frac{\gamma-1}{\gamma}}=\frac{\gamma+1}{2}$$

These equations contain only γ as a parameter. Furthermore, we find that for "reasonable" values of γ the basic character of the curves of $\frac{u}{u_*}$, $\frac{p}{p_*}$ and $\frac{\rho}{\rho_*}$ versus $\frac{A}{A_*}$ are unchanged by changes in γ. These curves have been sketched in figure 2. (The theory of perfect gases gives the result that $\gamma = 1+\frac{2}{n}$ where n is the number of degrees of freedom of the molecule. For real gas mixtures, "reasonable" γ's lie in the range between 1 and 2.)

All of the curves have the same general shape. They pass through the point (1, 1) with a vertical tangent at this point. They have two legs extending to the right, one assymptotically approaching the $\frac{A}{A_*}$ axis and the other approaching a horizontal assymptote having an ordinate greater than unity. Changes in γ affect only the rate of approach to the assymptotes and the levels of the upper assymptote.

Note that in figure 2 we have plotted the dependent variables u/u_*, p/p_*, and ρ/ρ_* against the independent variable A/A_*. In this form, the data are not single valued, but rather for every value of the area ratio, A/A_*, there are <u>two</u> possible values for each of the other variables. This fact will loom importantly in what follows.

The simplicity that we have achieved in eliminating B, χ and ϕ is not without its price. These constants are in reality constants of integration and we can not determine the basic scales of the problem until we have fitted these constants to the appropriate boundary conditions.

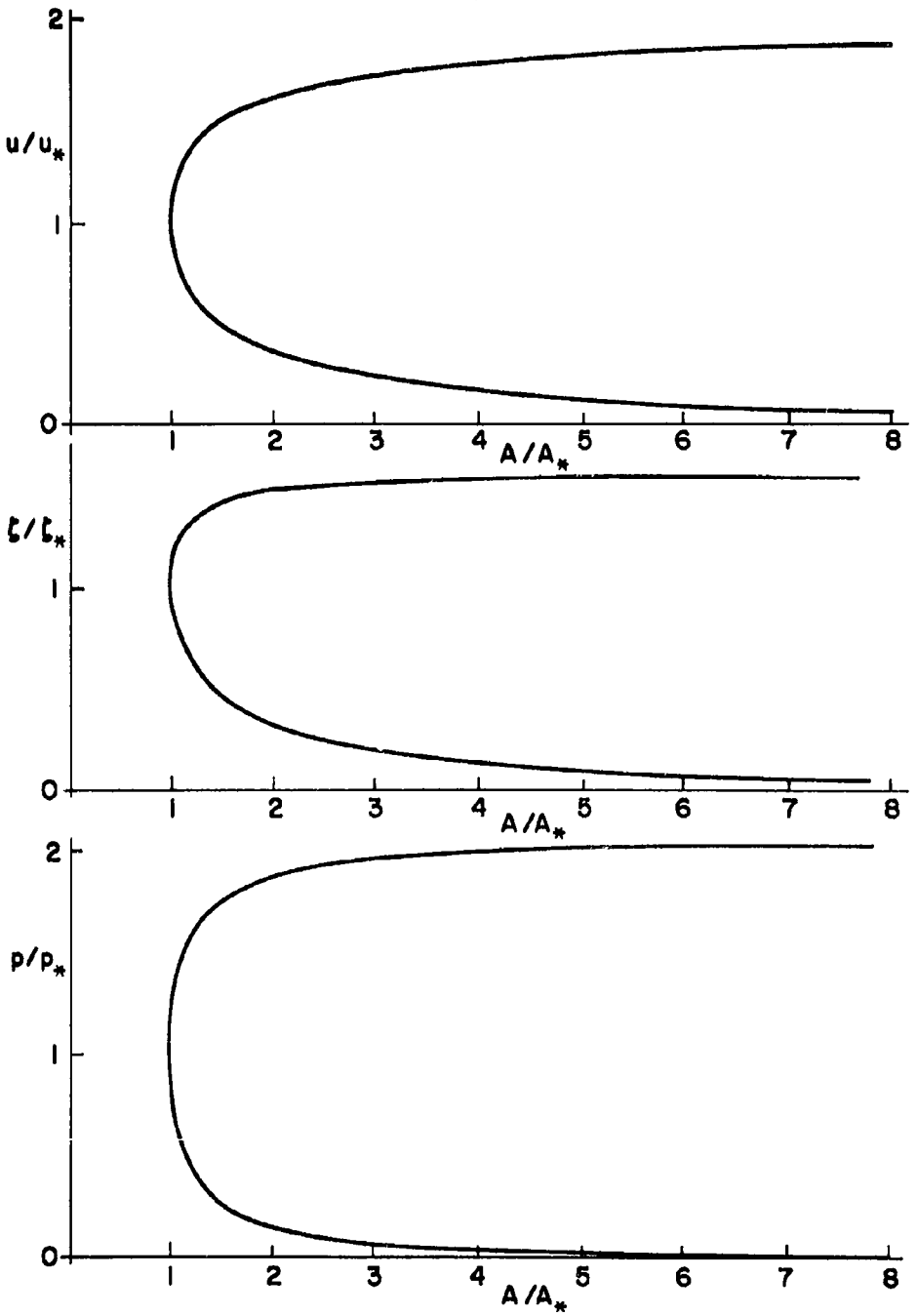

Figure 2

Returning now to figure 1, let us begin our considerations by supposing that a relatively small flow is passing from the lower container to the upper reservoir. Since ϕ is the magnitude of the flow and since $A_* = \Phi/(\rho_* u_*)$, a small value of ϕ relative to u_*, ρ_* and the areas A_L, A_T and A_E of the problem implies that A_* is small compared to these areas. Consequently, the ratios, A_L/A_*, A_T/A_* and A_E/A_* will be large, and thus will lie well to the right in the graphs of figure 2. With the proportions we have chosen, they will appear in much the way we have shown in figure 3.

Now let us increase the amount of the flow, with a corresponding increase in the scale area, A^*. The points will move to the left as shown in figure 4. This increase in flow corresponds, as it should, to a greater difference in pressure between the stations L and E. But now with the progression of change from figure 3 to figure 4, we see an interesting problem looming ahead. As we increase the flow, increasing A_* and moving the three points A_T, A_E and A_L toward the vertical tangent at $A/A_* = 1$, we see that long before either of the end points, A_L or A_E, experiences difficulty, the throat point, A_T, will reach $A/A_* = 1$ and will have no further place to go in its movement to the left. Now it is not enough to have a proper curve between the end points, A_L and A_E. The flow goes from A_L to A_E, but it does so by going from A_L to A_T and back to A_E. And it is of course essential that a real curve exist at A_T.

Our present line of reasoning has led us to a set of flows corresponding to increasing pressure differences, $p_L - p_E$, in the sequence, figure 3 through figure 4, to the limiting case of figure 5. We also see that the isolated case of figure 6 is possible. In this figure, the flow takes advantage of the fact that A_T is located at the vertical tangent and crosses to the second branch of the curves for the flow downstream of the throat. In so doing, it passes from subsonic speeds upstream from the throat through sonic speed at the throat to supersonic speeds downstream

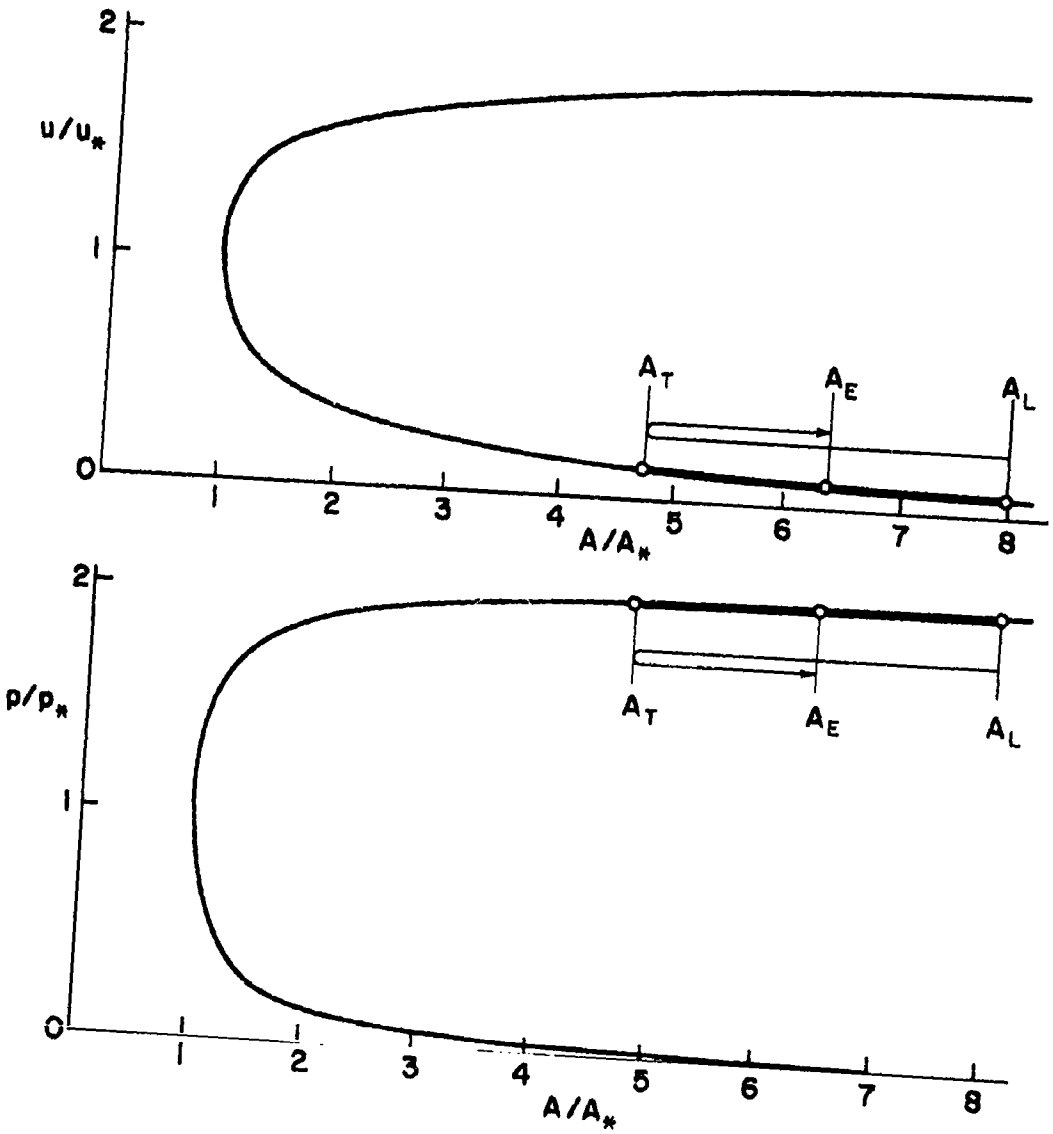

Figure 3

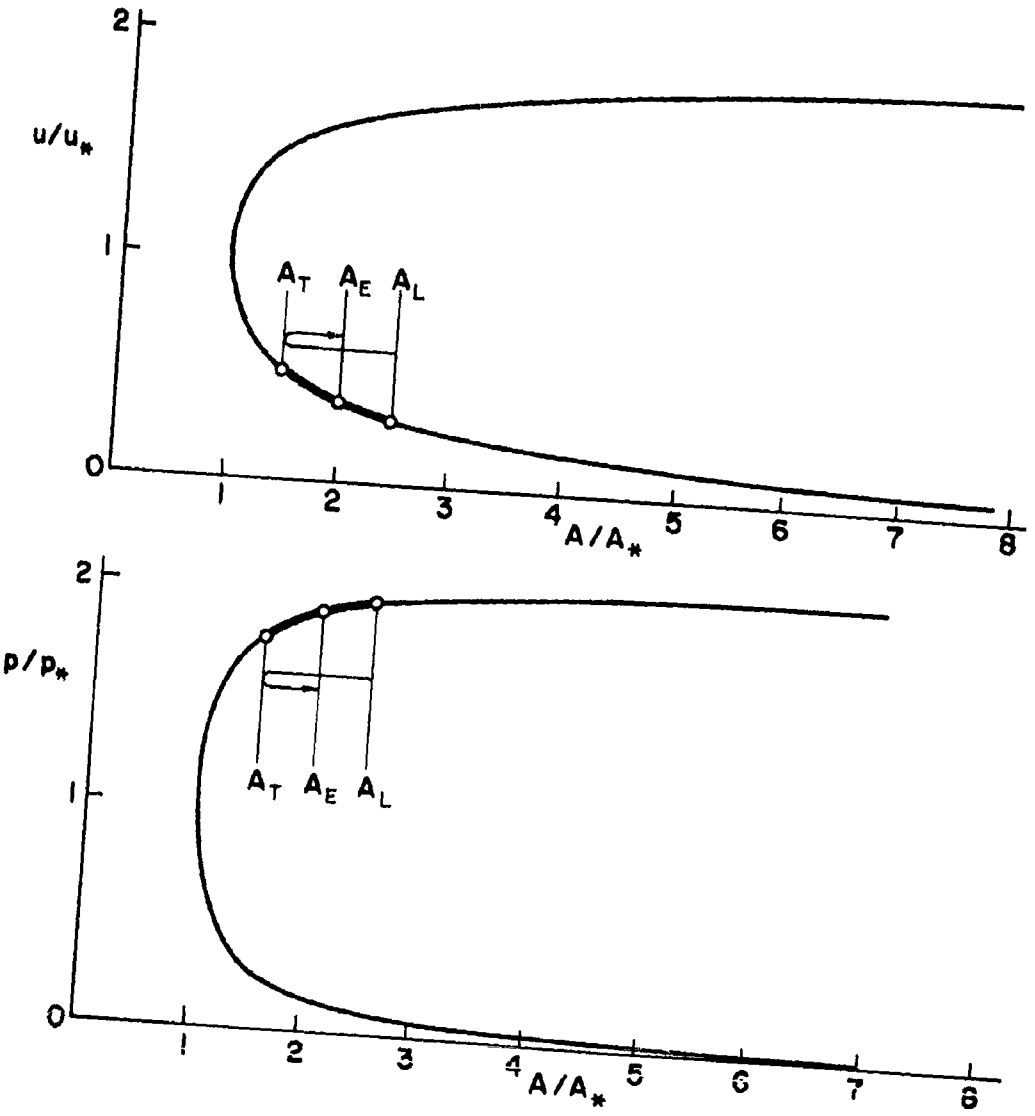

Figure 4

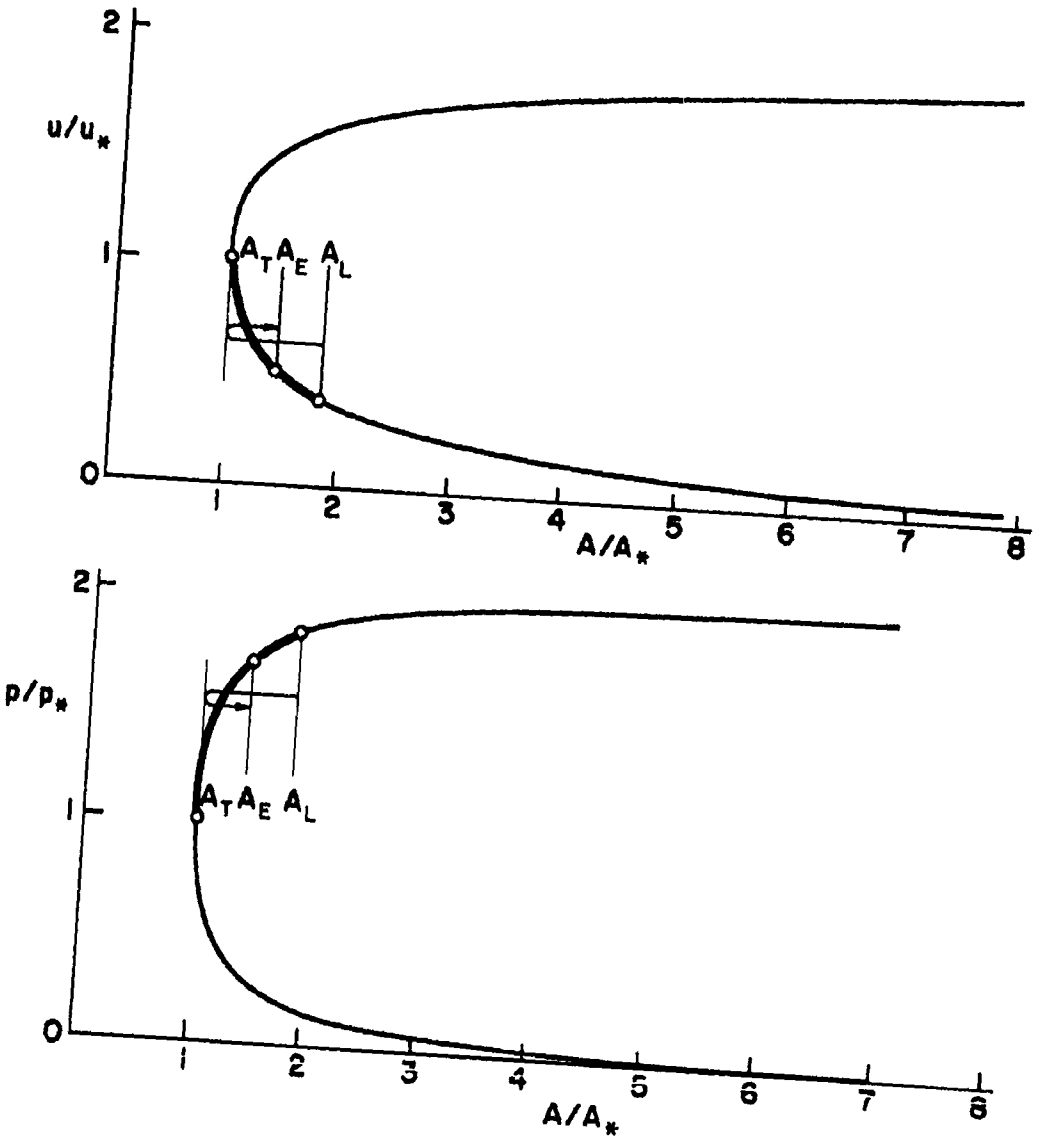

Figure 5

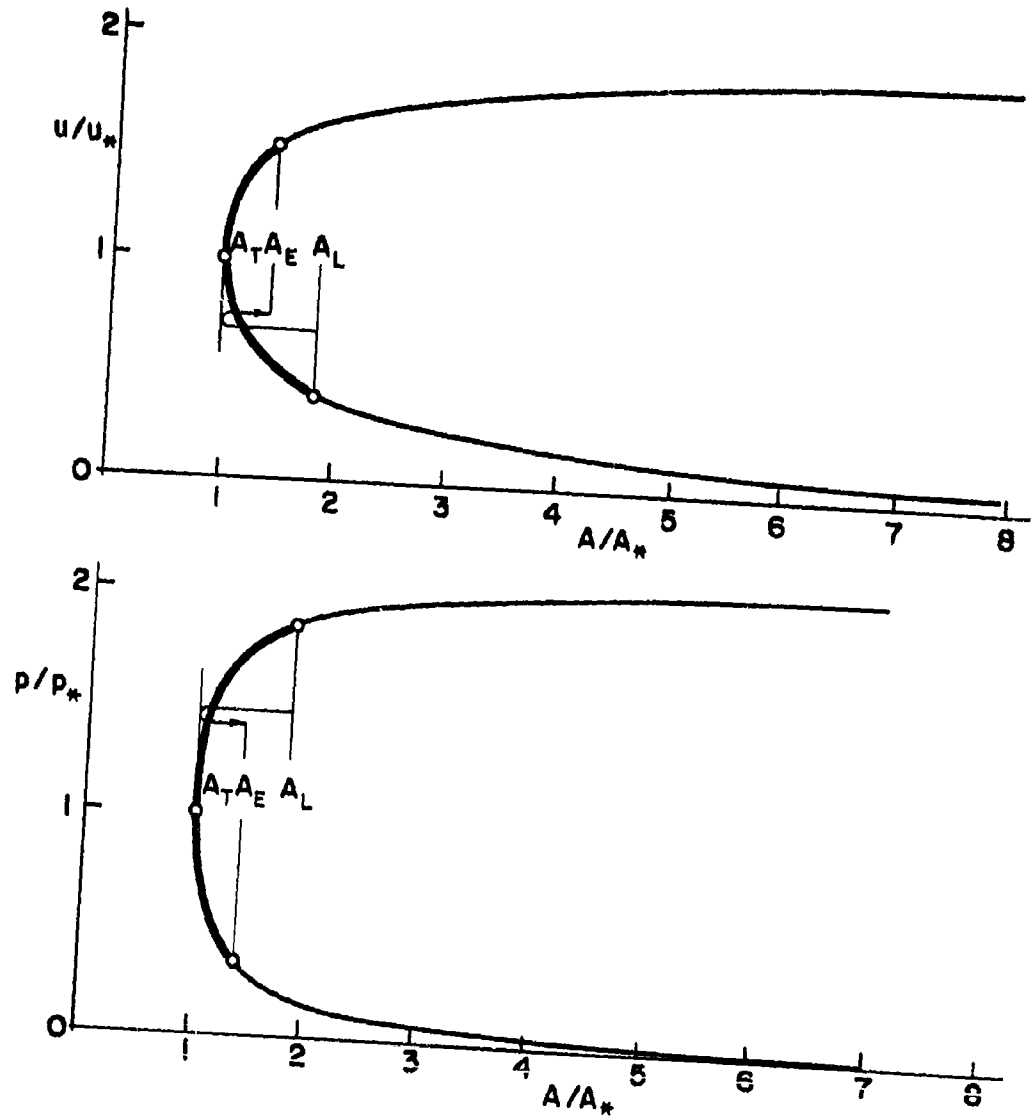

Figure 6

from the throat. In this isolated case, the pressure difference has jumped to a larger value.

We are now confronted with the following dilemma. In practice, we can set any pressure difference we want between the lower and the upper chamber. However, we have succeeded only in obtaining solutions for moderately small pressure differences and for a very special large pressure difference. What about the solutions for all the other pressure differences? One can readily verify that we have not overlooked solutions to the equations with which we started. Furthermore, the equations are right, as far as they go.

The answer to this dilemma lies in the fact that we have explored only continuous solutions. As frequently happens with nonlinear phenomena, the complete picture of behavior can only be obtained by taking into account discontinuous solutions as well. What happens is this. At the outset, we knew that the flow phenomena would be affected by viscosity and heat conductivity. A casual estimate showed that for all "normal" circumstances, their influence would be completely negligible. Since our work would be prohibitively complicated by including viscosity and heat conductivity, there was adequate justification for ignoring these factors. However, a closer examination shows that by ignoring them, we have reduced the order of the differential equations for the system and have thereby lost constants of integration and associated patterns of behavior. When the viscosity and heat conductivity are extremely small, the complete pattern of behavior is as follows. There is a backbone set of solutions which are almost everywhere indistinguishably close to the continuous solutions we have discussed earlier. In addition, there is a set of smooth but rapid transitions from supersonic to subsonic flow which have no counterpart in our earlier continuous solutions. As the viscosity and heat conductivity become vanishingly small, these abrupt transitions degenerate into discontinuous jumps which appear in nature as shock waves. These shock waves give us the added freedom needed to complete the picture of the

flows that accur for various pressure differences between the two containers of figure 1. In practice we need not consider the details of these "lost" transition solutions, but we must include shock jumps as part of our flow pattern if we are to predict the full range of flow behavior.

Let us consider a pressure difference that is a little greater than that corresponding to figure 5. Using this new degree of freedom afforded by shock waves, we find that the flow starts at subsonic speeds at A_L, becomes sonic at the throat, A_T and then, after becoming supersonic, experiences a shock at A_S which decelerates the flow to subsonic speed again. The flow then continues on, arriving at A_E at an even lower speed.

This sequence of events is shown in figure 7. At the shock, the mass flow, the momentum and the energy of the flow will be conserved. If subscripts 1 and 2 designate the states just before and just after the shock, then these conservation laws can be written

$$\rho_1 u_1 = \rho_2 u_2$$

$$p_1 + \rho_1 u_1^2 = p_2 + \rho_2 u_2^2$$

$$\frac{u_1^2}{2} + \frac{c_1^2}{\gamma - 1} = \frac{u_2^2}{2} + \frac{c_2^2}{\gamma - 1}$$

Here, we must pay an additional price for the simplicity we gained by using the scale factors u_*, p_*, ρ_* and A_* in our plotting procedure. If we insert these factors in the above relations, we find that while u_* is unchanged in crossing the shock, both p_* and ρ_* decrease and A_* increases. Thus we must always make a change in scales as we cross the shock.

When p_E is only slightly less than that corresponding to figure 5, the shock wave of figure 7 will be located very close to the throat. The

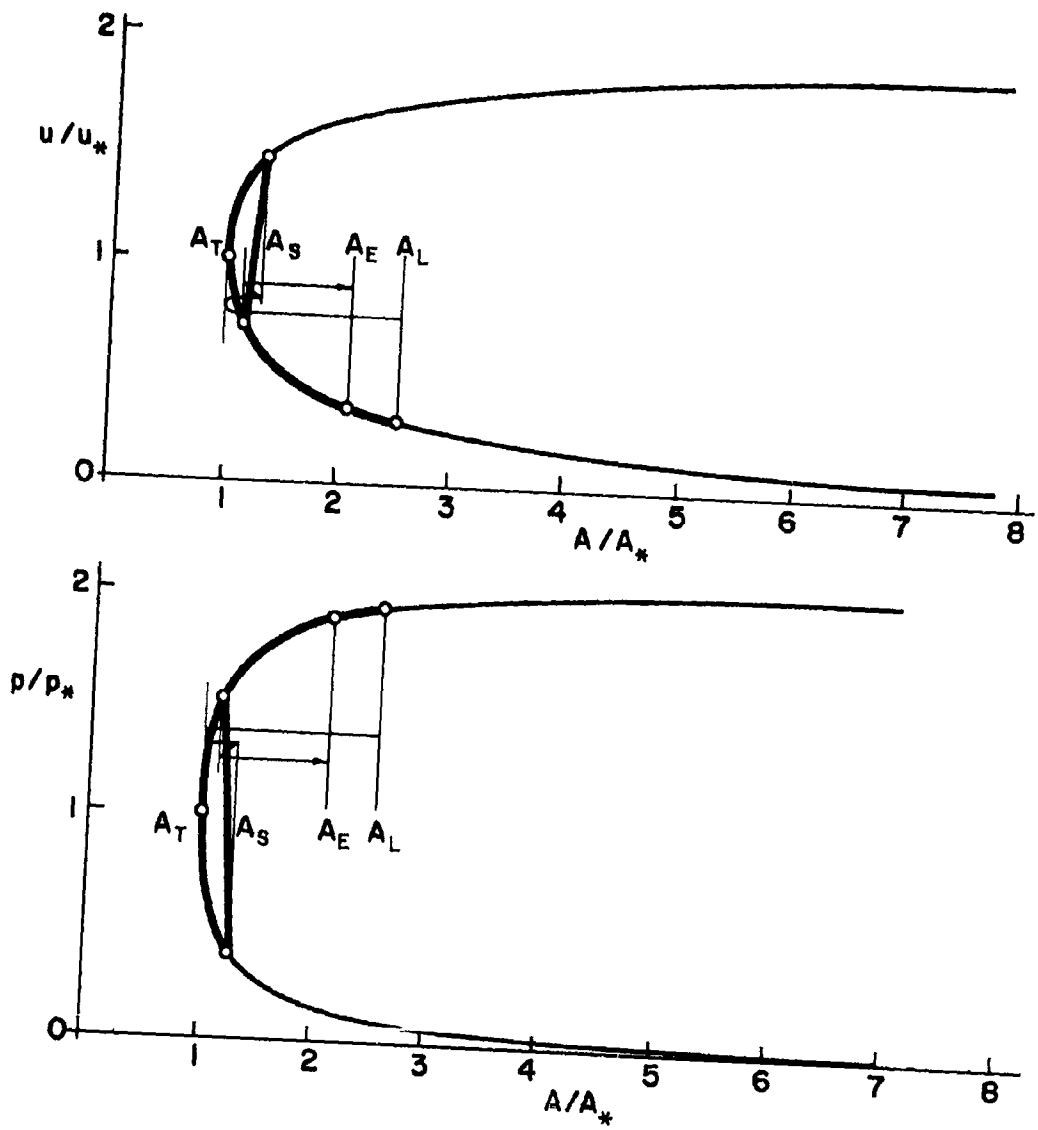

Figure 7

jump across the shock wave will be small and the changes in p_*, ρ_* and A_* will be correspondingly small. Thus the flow will closely resemble that of figure 5 except for the small supersonic region and the shock wave located just downstream from the throat. Consequently, this new class of flows forms a smooth continuation of the class of flows we found earlier.

As the pressure, p_E, is lowered, the shock wave of figure 7 moves downstream and becomes stronger until it stands at the exit station, E, as shown in figure 8. During this movement of the shock wave from the throat to the exit station, the entire upstream flow appears to be frozen in its pattern, i.e. it is completely unaffacted by changes in p_E. All that happens is that a greater portion of this flow becomes supersonic. When this occurs the flow is said to be "choked". The shock wave then becomes the dominant actor in the changing pattern of the overall flow.

If we consider lower values of p_E that of figure 8, we are no longer able to maintain our assumption that the flow is essentially one-dimensional, i.e. that it is essentially constant across the flow. For such values of p_E, the entire flow in the pipe appears to be frozen in its pattern, and the principal action that takes place is the change of the normal shock wave into diagonal shock waves anchored at the edges of the exit section as shown in figure 9. As the pressure p_E is lowered, these shocks turn downstream and become progressively weaker. When p_E reaches the value corresponding to that of figure 6, the shocks stand at the Mach angle, $\sin^{-1} \alpha/\mu$, and have decreased to zero strength. For still lower values of p_E, the shocks are replaced by expansion waves. Thus, the case of figure 6, which was previously an isolated case, now fits into the progressive scheme of flow pattern changes.

We have now succeeded in obtaining a picture of the flow pattern for the full range of pressure differences that cause fluid to move from the lower to the upper container of figure 1, and by a simple extension of these ideas, the corresponding patterns for flows in the other direction can be obtained.

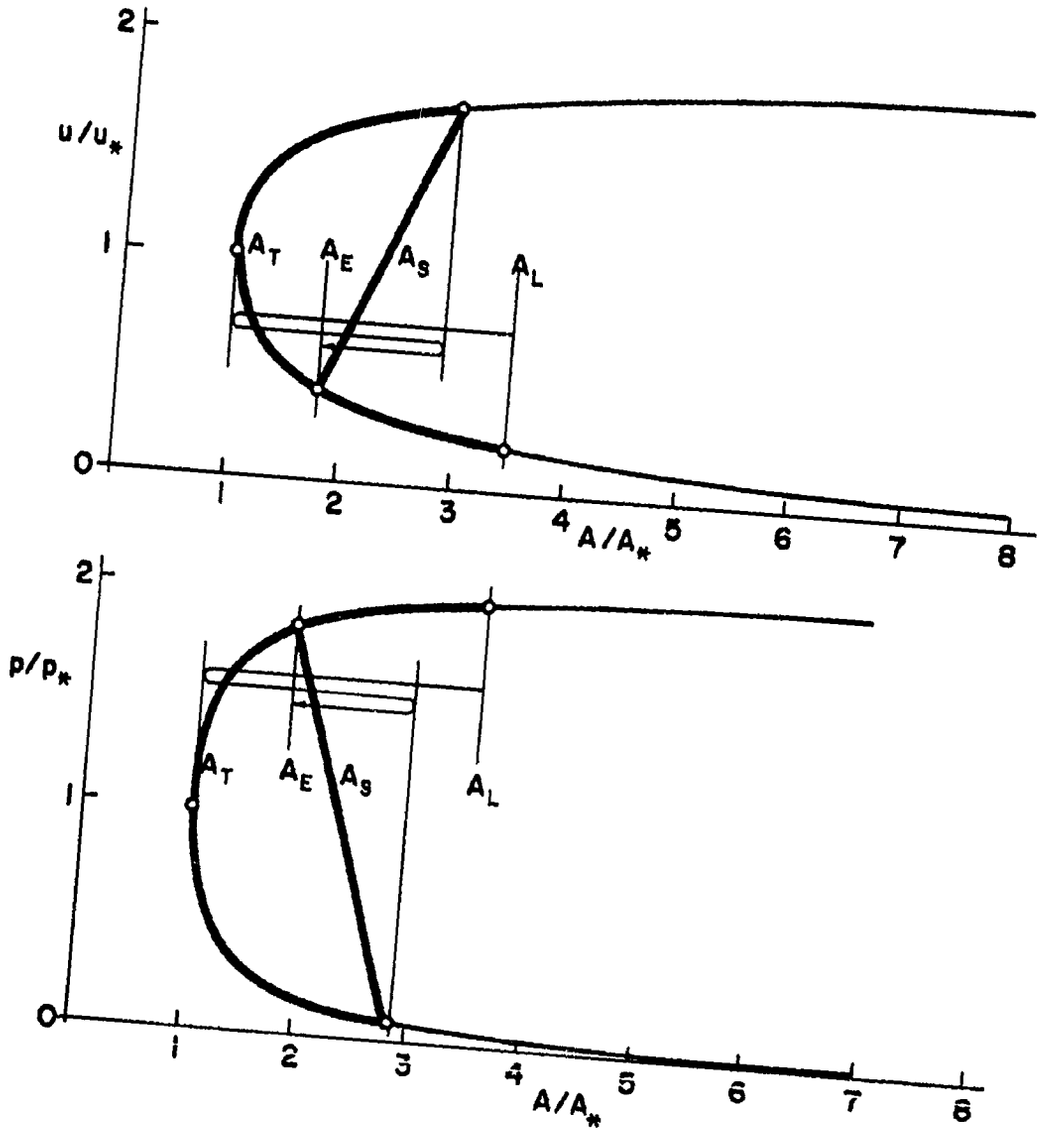

Figure 8

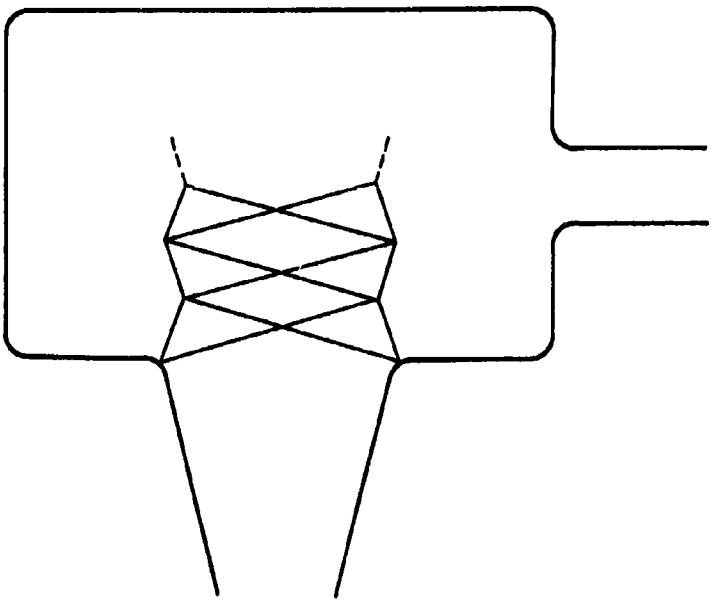

Figure 9

In summary, we have found that for small pressure differences, the flow will be subsonic everywhere, but as the downstream reservoir pressure is decreased, the flow quantity will increase until sonic velocity occurs at the throat. At this point, the flow is choked and no further increase in flow quantity can take place. The subsonic flow upstream from the throat becomes frozen. Further decrease in the downstream reservoir pressure causes supersonic flow to appear downstream from the throat. This supersonic flow is terminated by a shock wave and the remaining stretch of flow to the downstream reservoir is subsonic. The shock first appears at the throat, and as the downstream pressure is lowered the shock moves downstream. It eventually enters the downstream reservoir where it divides into a diamond pattern of diagonal waves.

The Dynamics of Spherical Flows Having a Gravitational Field

Now let us attack the problem of the flow into and away from a star. We shall consider the flow field to be spherically symmetrical. Consequently, for purposes of comparison with our previous work, we may consider a representative segment of the flow as shown in figure 10. We begin by noting the points of similarity and difference between the flows of figures 1 and 10. In the case of the star, the thermonuclear reaction serves the same role as the heat source in the pipe flow. The mass of the star is sufficiently great that, for the time scales in which we are interested, it can play the role of providing an indefinite amount of material to the "boiling" liquid. The activity in the corona will correspond to the boiling process and the coronal surface will correspond to the level just above the surface of the liquid. The interstellar medium, with its pressure, p_M, will correspond to the upper reservoir of figure 1 with the corresponding pressure, p_R.

Previously, the upper and lower chambers were connected by a pipe with a minimal area in between; now the two "chambers" are connected by a "conduit" with continuously increasing area. In addition, we now have

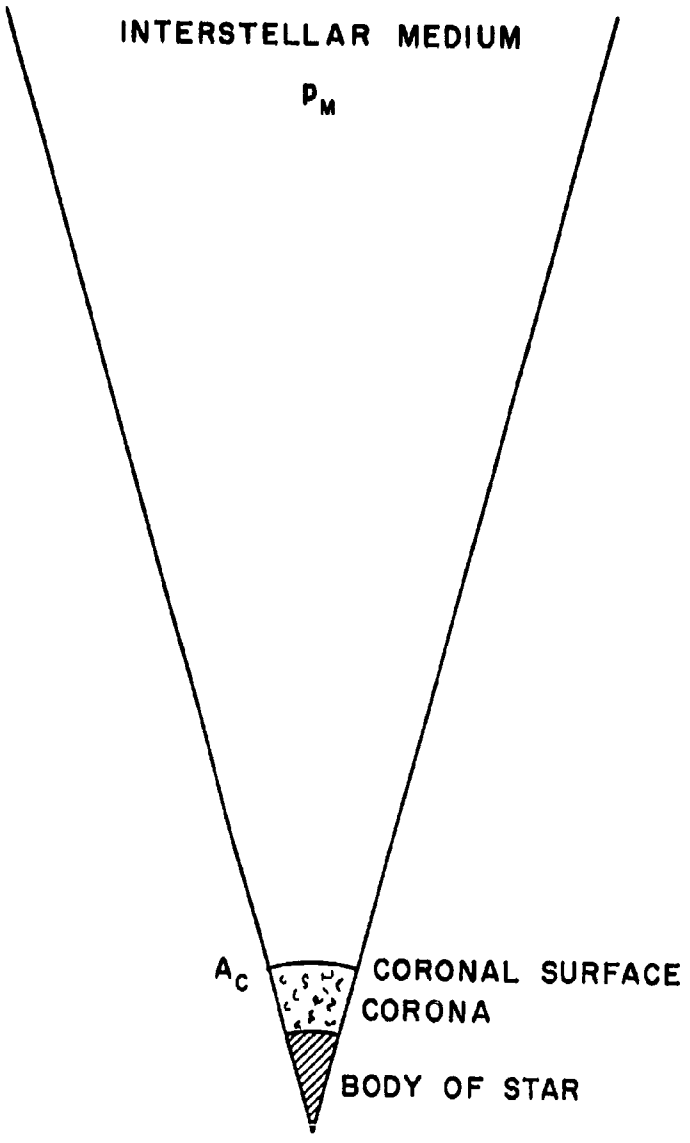
INTERSTELLAR MEDIUM
p_M
A_C
CORONAL SURFACE
CORONA
BODY OF STAR

Figure 10

the star's gravitational field acting upon the flow. Later we shall see that the effect of this field is not unlike that of a throat in the flow.

Again, we shall investigate the full range of flow patterns for all possible values of the interstellar medium pressure, p_M . The equations $\rho u A = \phi$, $p = K \rho^{\gamma}$, $C^2 = \gamma p/\rho$, which we used previously, remain unchanged. To the Bernoulli equation must be added a gravitational term, thus: $\frac{u^2}{2} + \frac{C^2}{\gamma - 1} - \frac{G M}{r} = B$.
Here, M is the mass of the star, G is the gravitational constant and r is the radius of the section under consideration. The addition of the gravitational term means that the Bernoulli constant, B , can now be negative. When this is true it indicates that the kinetic energy and the thermal energies are numerically less than the potential energy.

We must make a change in the independent variable of the problem. Previously we used the area of the cross-section as the independent variable because the distance along the flow path did not enter the equations directly. Now, this distance, r , does enter directly (through the gravitational term) and we shall use it as an independent variable. The cross-sectional area, A , for a sector of one ster-radian, is related to r by the formula: $A = r^2$.

As before, we may simplify our problem of examining all solutions of these equations by incorporating the constants, B , ϕ , G , M and χ into scale factors. Previously, we succeeded in eliminating all of the constants of integration and ended up with a single curve for each value of the thermodynamic parameter, γ . Now, we are not able to eliminate all of the constants of integration, but end up with a single combined integration constant which we shall call λ .

For convenience, we define our dimensionless variables in the following way:

$$W = \frac{u^2}{2|B|}$$

$$R = \frac{r|B|}{G_1 M}$$

$$P = \frac{p K^{\frac{1}{\gamma-1}}}{|B|^{\gamma/\gamma-1}}$$

$$\lambda = \frac{|B|^{\frac{3\gamma-5}{\gamma-1}} \Phi^2 K^{\frac{2}{\gamma-1}} \left(\frac{\gamma}{\gamma-1}\right)^{\frac{2}{\gamma-1}}}{2 G_1^4 M^4}$$

If we eliminate all the other variables except W and R and obtain a single equation relating this velocity variable, W to the radius variable, R, we have:

$$W - \frac{1}{R} + \left(\frac{\lambda}{W R^4}\right)^{\frac{\gamma-1}{2}} = \pm 1$$

We notice that we must divide our analysis into two parts; one for use when B is positive and another for use when B is negative. These correspond to the two states of positive and negative total energy, with a corresponding sign for each on the right side of the above equation.

Previously, we obtained a single curve for all flows having the same γ, and all of the different γ curves had essentially the same shape.

Now, there will be a family of curves for each value of γ, each member of the family corresponding to one value of λ. Furthermore, the different members of a given family will have essentially different shapes and the different families will be essentially different in their grouping of curves in the family.

In practice, we shall be interested in values of γ that range from $\gamma = 1$, which corresponds to a gas which is rendered isothermal by virtue of great internal energy storage (e.g. high molecular weight), great heat conductivity, or other similar causes, up to a value of $\gamma = \infty$

which corresponds to a gas having no interaction between its particles (i.e., they are locally free particles). Within this range of γ, the above equation relating W to R behaves differently in the subranges $1 < \gamma < 3/2$, $3/2 < \gamma < 5/3$ and $5/3 < \gamma < \infty$.

Let us first examine the simple case of a non-interacting gas with $\gamma = \infty$. In this case, $W - \frac{1}{R} = \pm 1$, and the constant of intergration, λ, has been entirely eliminated. This equation has been plotted in figure 11 for both positive and the negative energies. It will be seen that for the positive energy case, the particles never have values of the velocity parameter, W (or kinetic energy parameter) less than unity in the coordinates we are using. Similarly for the negative energy case, the radius parameter, R, never exceeds the value unity.

For a gas with interacting particles, let us first consider the case for which $\gamma = 2$. Such a gas has relatively little internal energy storage. (It corresponds to a gas having only 2 degrees of freedom, i.e. with perhaps one of the translation degrees being eliminated by means of a magnetic field.) This case has been plotted in figure 12 for positive energies and in figure 13 for negative energies. Instead of having single curves for each case, we have families of curves for various values of λ, which is a dimensionless parameter giving the amount of flow coming into or going out from the star. Furthermore the velocity is no longer a single valued function of the radius, but rather each curve has two values of the velocity for each radius. If we examine the curves more closely, we find that the upper branch of each curve corresponds to supersonic flows with the Mach number, M being greater than one and the lower branch to subsonic flows with M less than one. The dotted lines of figures 12 and 13 show the loci of vertical tangents where the transition from subsonic to supersonic flow takes place. In this figure, and in those that follow, the equation for the locus of vertical tangents (the M = 1 line) is $W = \frac{\gamma-1}{\gamma+1}\left(\frac{1}{R} \pm 1\right)$.

The corresponding equation for the locus of horizontal tangents is

Figure 11

Free Particles ($\gamma = \infty$)

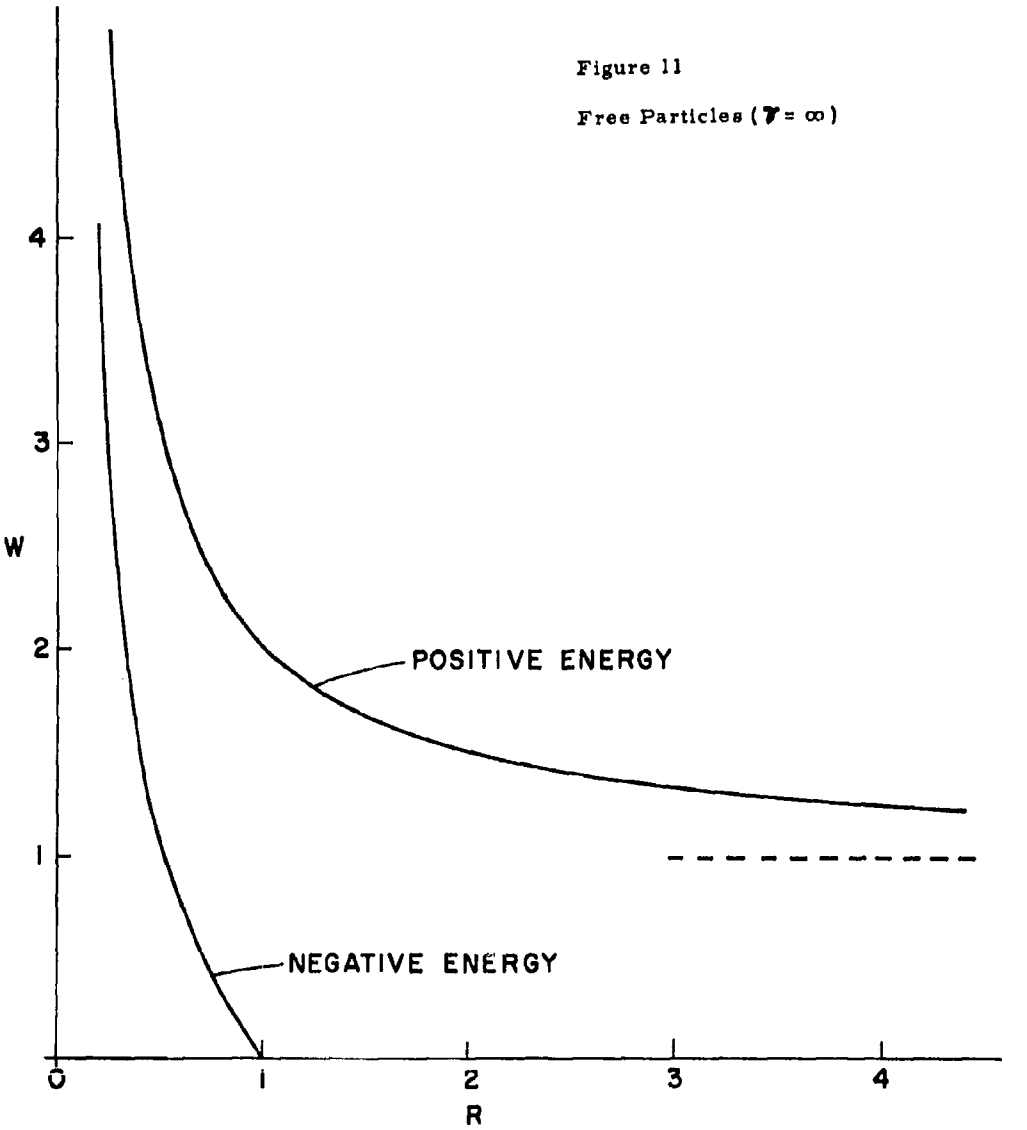

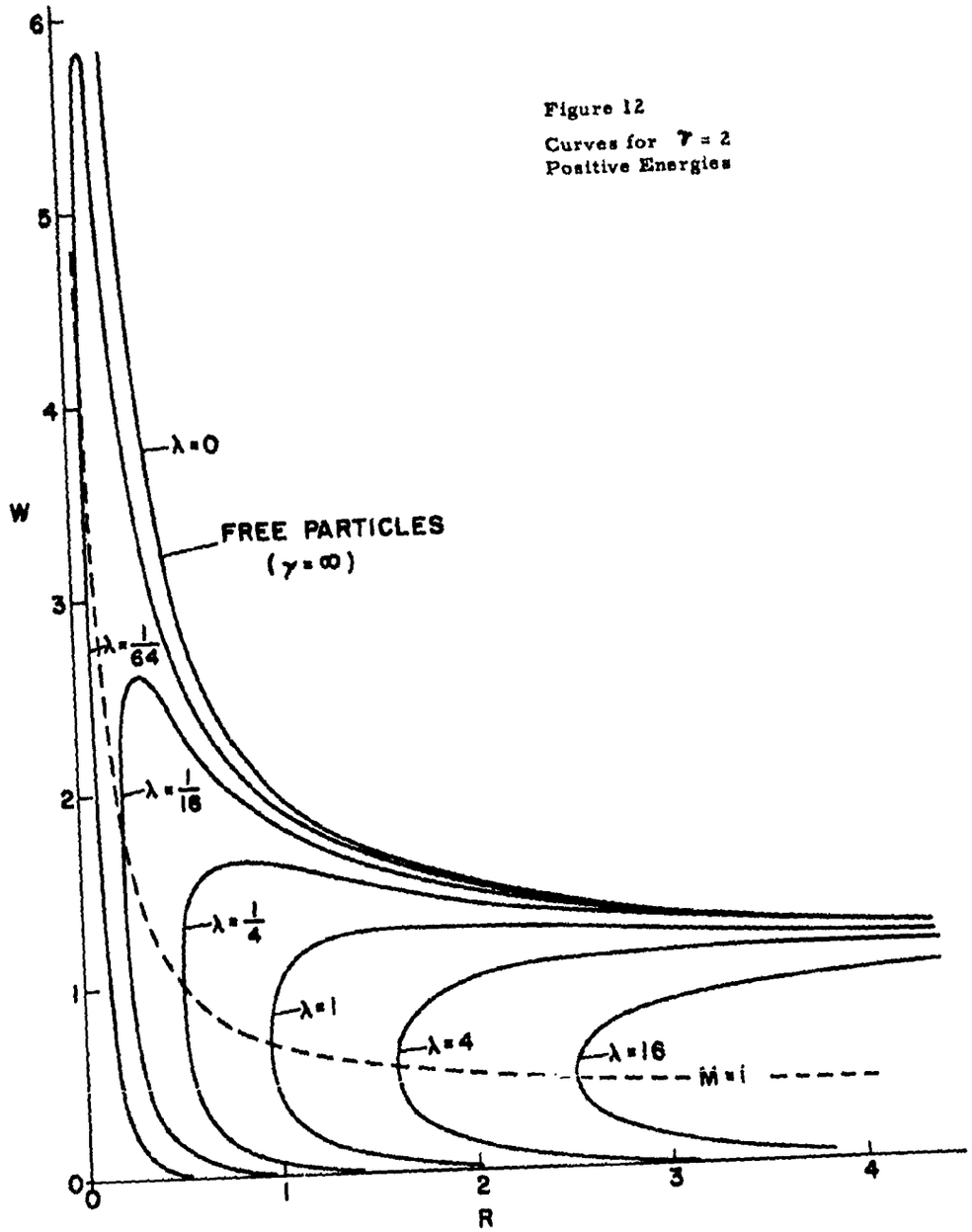

Figure 12

Curves for $\gamma = 2$
Positive Energies

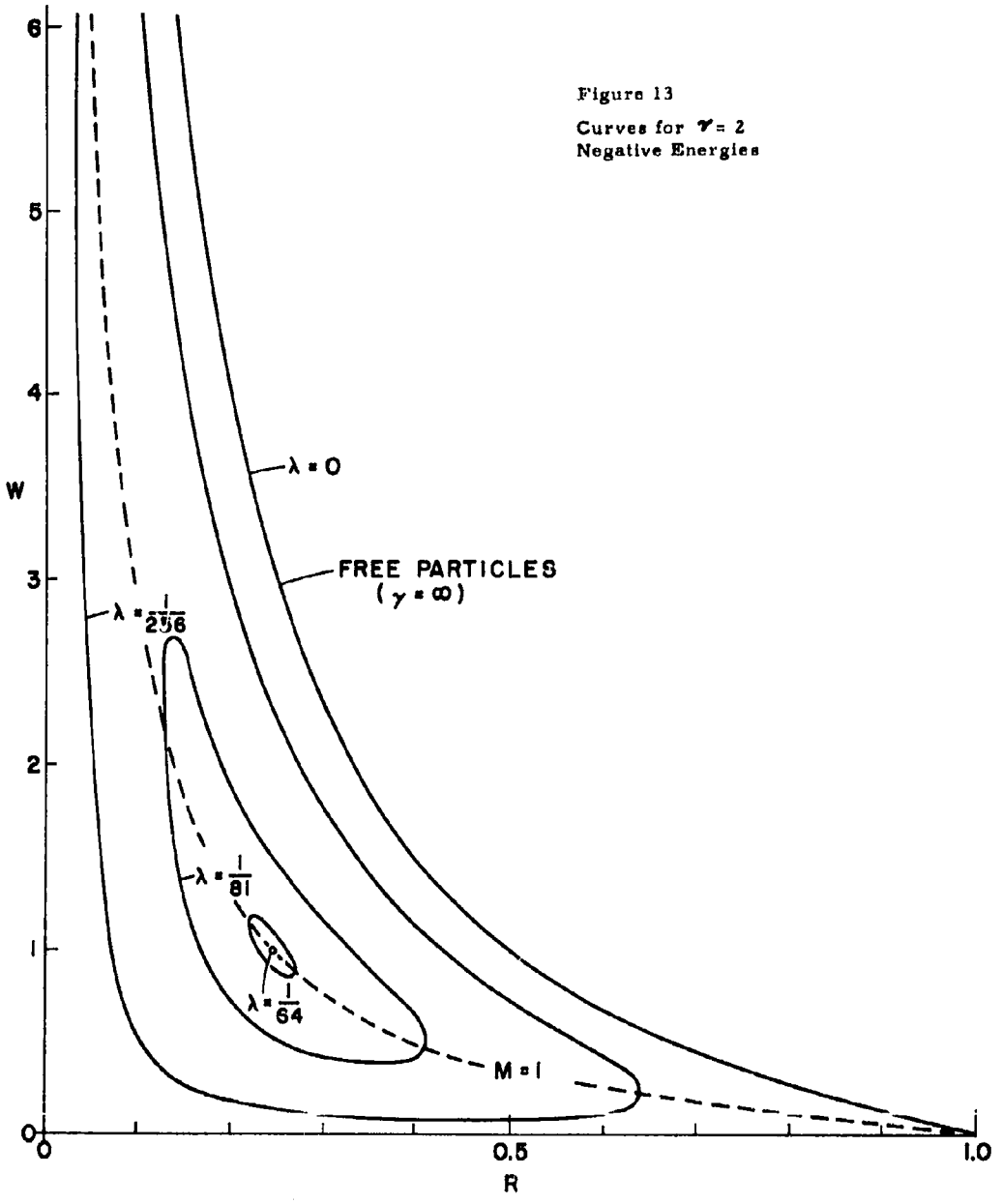

Figure 13

Curves for $\gamma = 2$
Negative Energies

$$W = \frac{2\gamma - 3}{2(\gamma - 1)} \cdot \frac{1}{R} \pm 1 \quad .$$

An interesting physical phenomenon now emerges. Suppose we were to follow a given positive energy flow in from great radius (the flow itself can either be going in or out). As we come in, we always reach a limiting radius where the curve says the flow doubles back on itself. Since this is physically impossible, it means that for each flow, there is a "choking" radius beyond which the flow simply cannot go. This choking phenomenon is in close analogy with the results which we have obtained earlier.

For the negative energy case, an even more interesting situation arises. The curves of figure 13 have a certain singular point. As a result, each curve passes through M = 1 twice. Thus, there is both an inner and an outer choking radius, i.e. a flow starts at sonic speed at one radius and travels outward at either subsonic or supersonic speeds according to choice, and again becomes sonic at an outer radius. Beyond these two the flow can have no real existence.

We notice another point which is common to both positive and negative energies; namely that for $\gamma = 2$, there is no physical way in which a transition from subsonic to supersonic flow can take place.

Let us consider flows with somewhat lower values of γ. As γ decreases, the essential character of the curves does not change until a value of γ equal to 5/3 is reached. Then, as shown in figures 14 and 15, the following situation exists. For positive energies, the curves still have the shape of a bent hairpin for values of λ between ∞ and $3^3/4^4$. However, for $\lambda = 3^3/4^4$, the sharp curve of the hairpin goes off to infinity and for values of λ between o and $3^3/4^4$ the curves divide into two sets, each having a hyperbola-like shape. One set lies close to the vertical axis and the other lies close to the free particle curve. For these two sets of curves, no choking occurs; one set is supersonic, the other subsonic; both exist throughout the full range of radii.

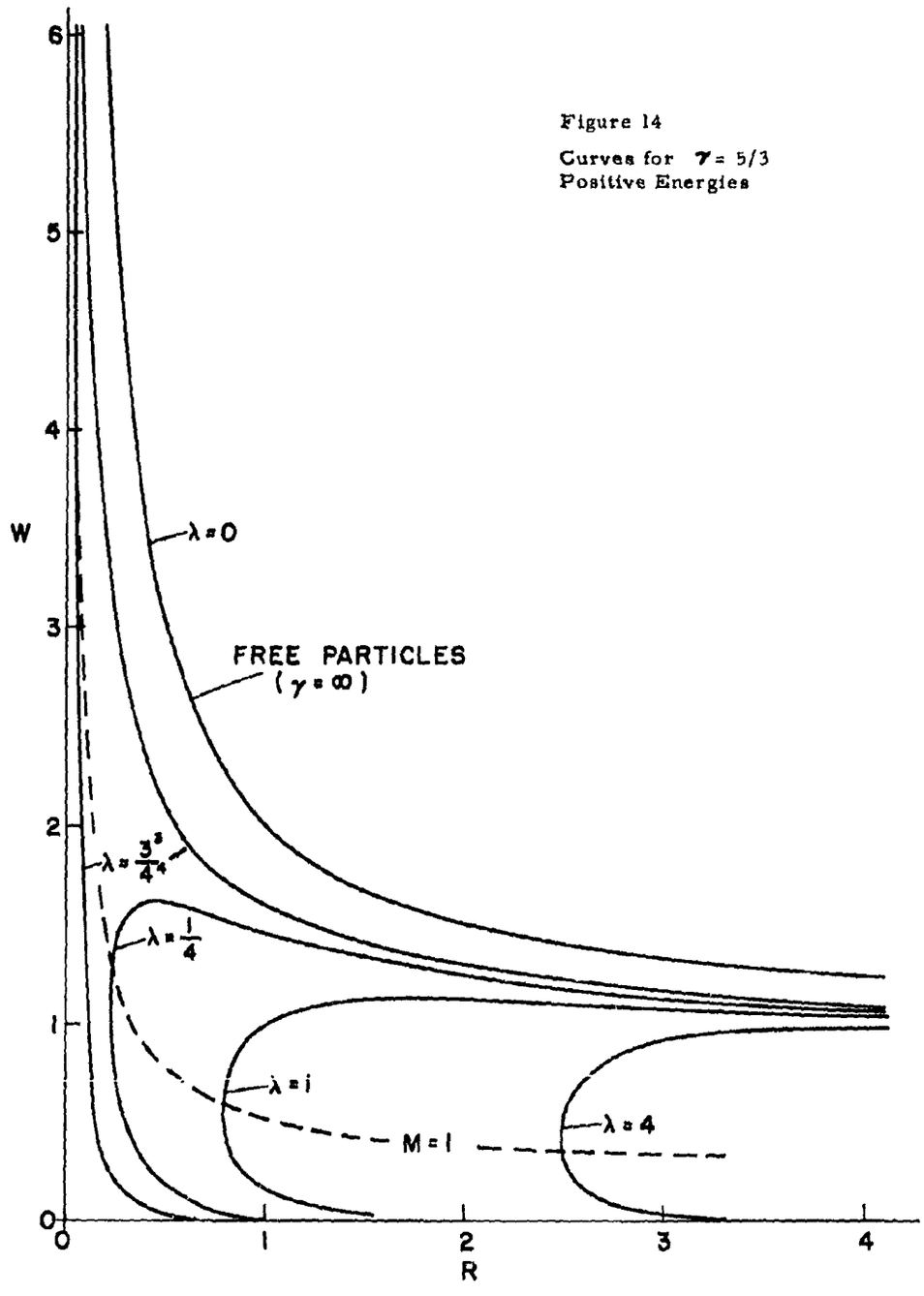

Figure 14

Curves for $\gamma = 5/3$
Positive Energies

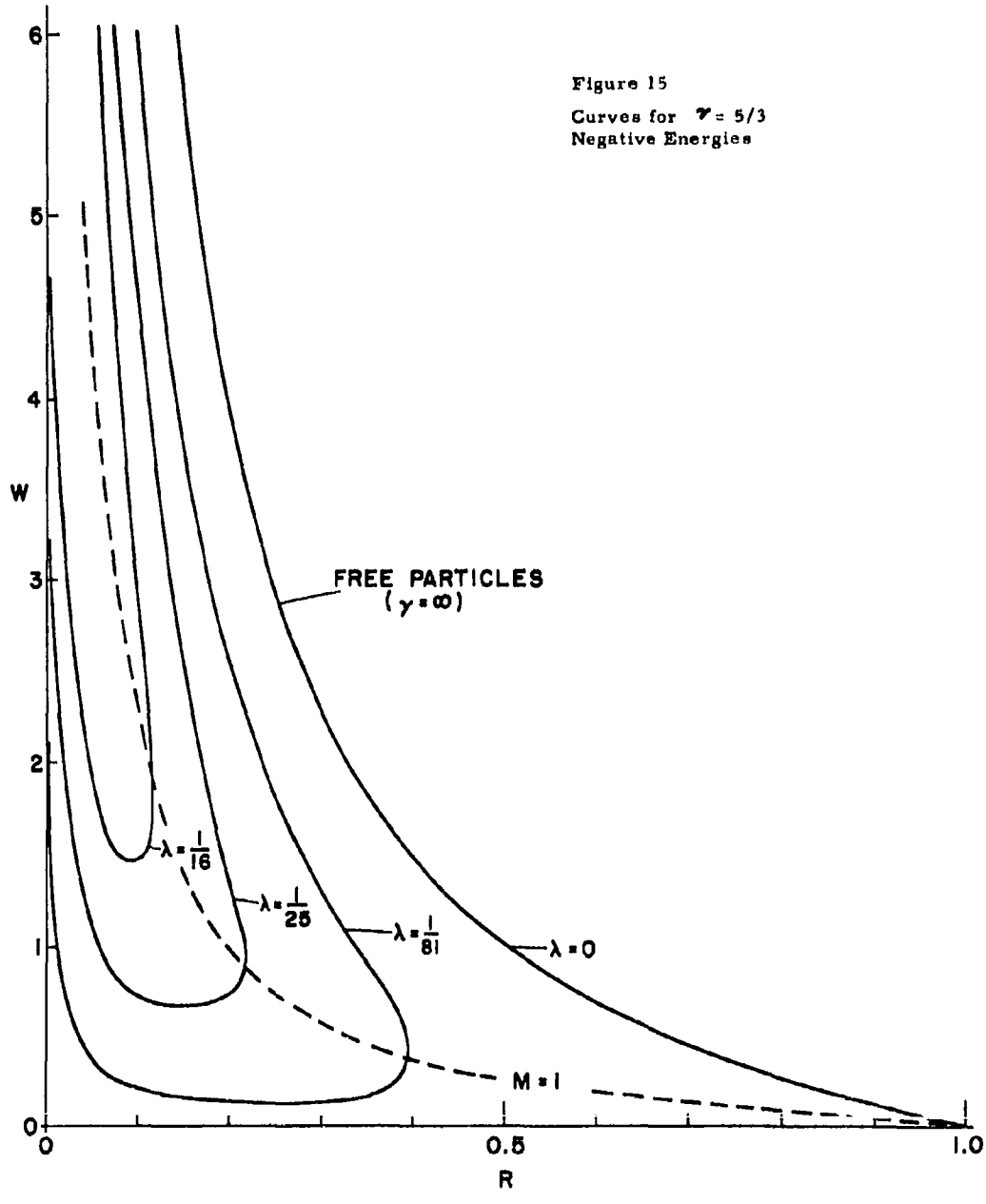

Figure 15

Curves for $\gamma = 5/3$
Negative Energies

For the negative energy cases the center singularity has moved off to $W = \infty$ and the curves now have a bent hairpin shape, open at the top. The choking of the flow occurs only at a limiting outer radius.

As we pass to lower values of γ ; the next major change in the character of the curves occurs at $\gamma = 3/2$. Between $\gamma = 5/3$ and $\gamma = 3/2$, the curves have the typical shapes shown in figure 16. A saddle singularity has appeared for the positive energy cases. This saddle singularity divides the field into 4 parts. In two of the parts, one subsonic and the other supersonic, the curves have hyperbola-like shapes which exist for the whole range of R's . The other two parts have bent hairpin shapes, one being open at the top, the other open to the right. These curves each have a limiting choking radius, one being an inner radius, the other an outer radius.

The curves of figure 16 for positive energies show one notable feature. For the first time, they offer the possibility of real, continuous transitions between subsonic and supersonic flows. These occur on the two branches of the saddle singularity. Such flows are quite analogous to the nozzle flows we encountered earlier. Here, the gravitational field serves to insert a nozzle in an otherwise monotonically expanding or contracting flow. It is likely that just as in the nozzle case, the flow from supersonic to subsonic speeds is unstable (shock waves appear). However, in figure 16, one branch of the saddle corresponds to subsonic to supersonic transitions in outward flows and the other to transition in inward flows.

For the special case of $\gamma = 3/2$, the curves have the shapes shown in figures 17 and 18. For positive energies, we still have the saddle singularity, but now the flows all start with finite subsonic velocities at $R = 0$. Some accelerate to supersonic speeds, passing through a limiting radius and doubling back on themselves. Others slow down, being permanently subsonic. At outer radii, there is a set of permanently supersonic flows and a set that makes a doubling back transition from subsonic to

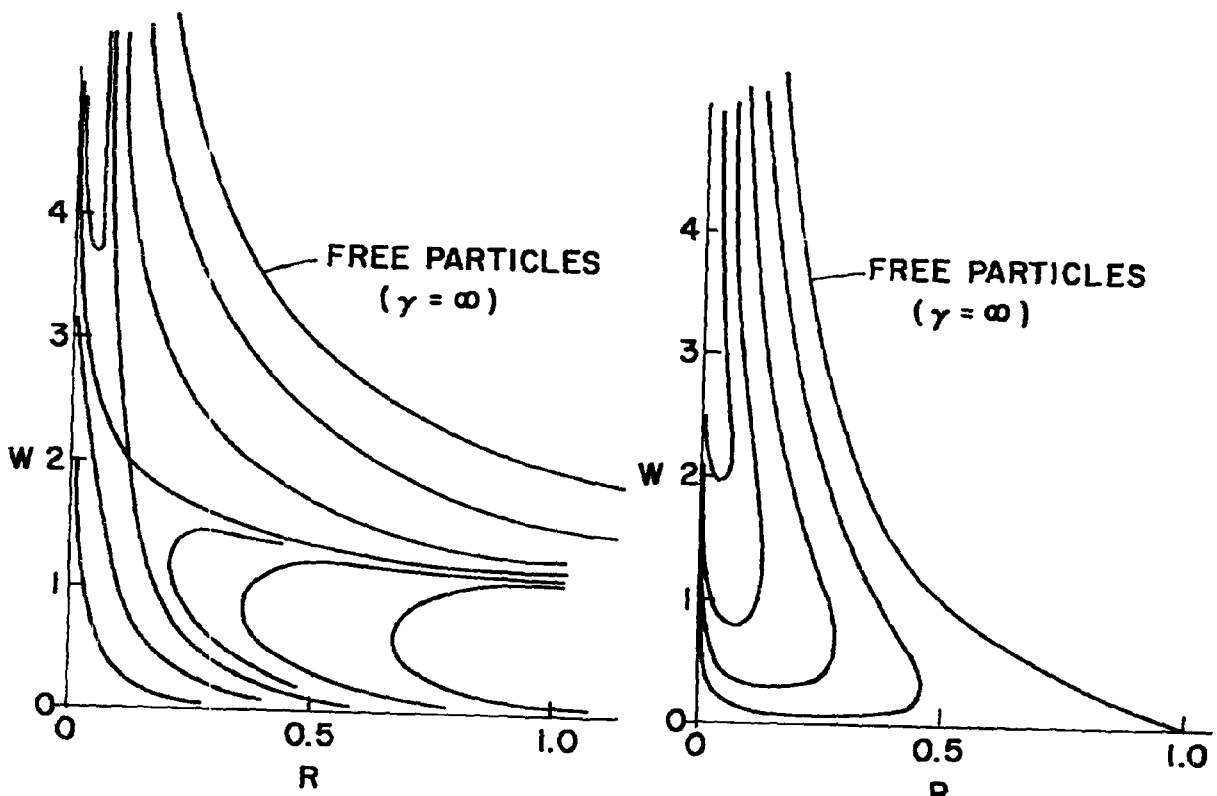

Typical Curves for $\frac{3}{2} < \gamma < 5/3$
Positive Energies

Typical Curves for $\frac{3}{2} < \gamma < 5/3$
Negative Energies

Figure 16

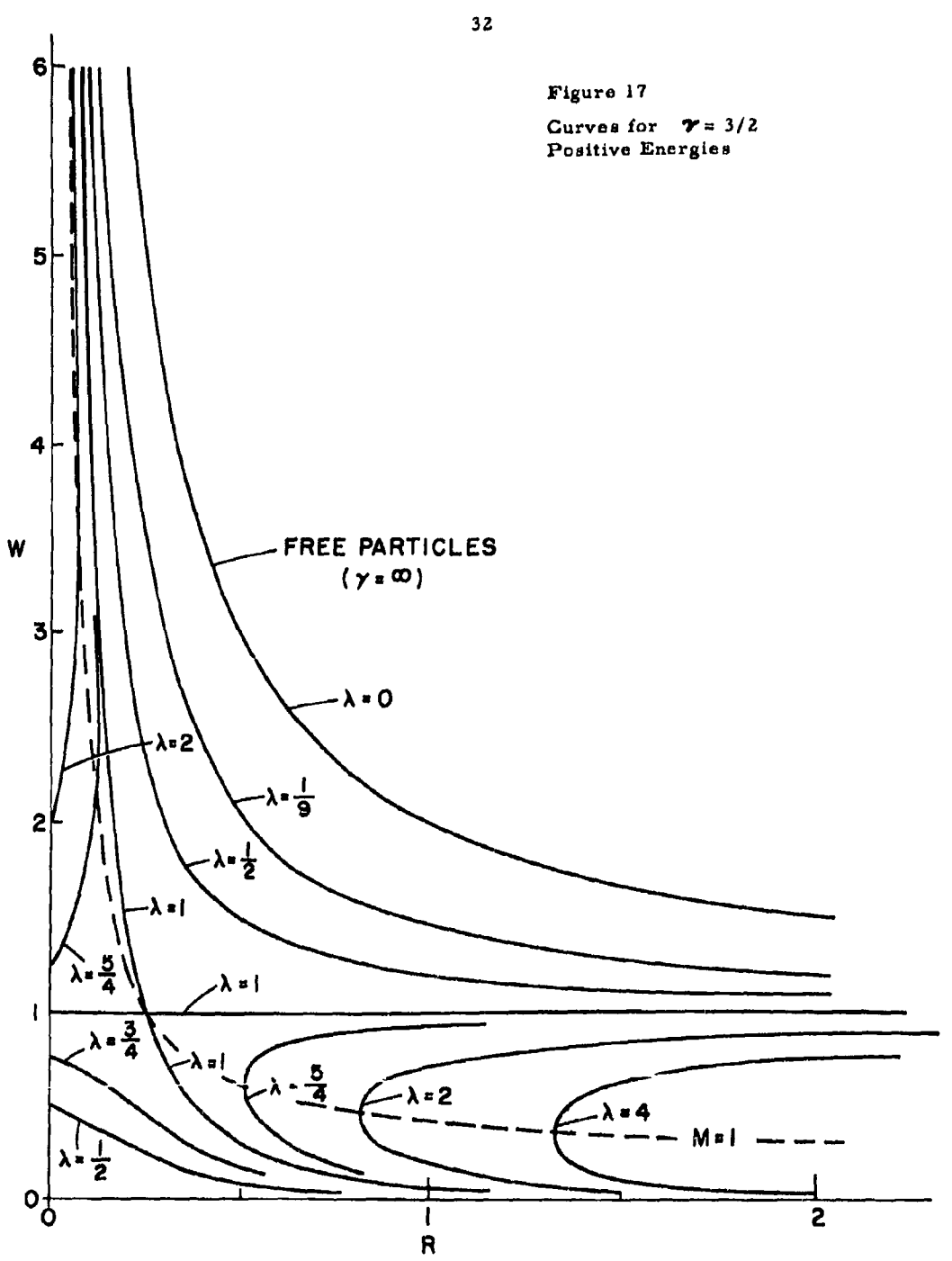

Figure 17

Curves for $\gamma = 3/2$
Positive Energies

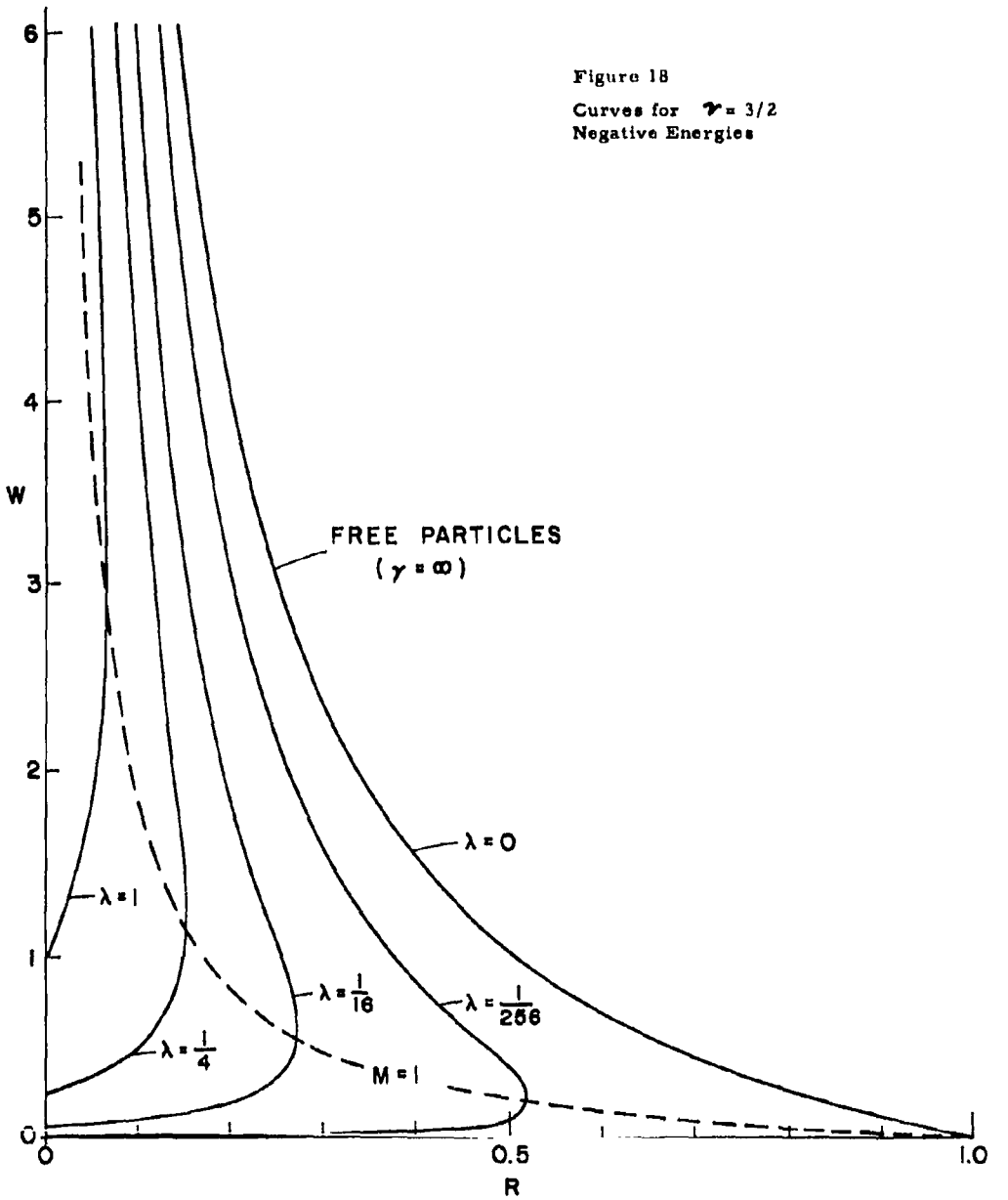

Figure 18

Curves for $\gamma = 3/2$
Negative Energies

supersonic speeds at an inner limiting radius. Perhaps the most interesting feature of figure 17 is the existence, for $\lambda = 1$, of a flow having a constant velocity as it expands outwards. In the process, the temperature drops, so that even though the flow velocity stays constant, the Mach number passes from zero to infinity.

For the negative energy case of figure 18, the curves again start at finite subsonic velocities at $R = o$. But here they all choke at limiting outer radii and turn back on themselves to supersonic speeds.

As we go to still lower values of γ, the next major change in shape of the curves occurs at $\gamma = 1$. Between $\gamma = 3/2$ and $\gamma = 1$, the curves have the typical shapes shown in figure 19. They resemble the curves of figures 17 and 18 except for the fact that at $R = o$ the curves start off with zero velocity instead of a finite velocity. The positive energy curves now give the possibility of starting at small radii with a flow having low velocities which are subsonic and accelerating this flow to supersonic velocities at greater radii. These curves also offer the inverse possibility; namely that of starting at great radii with low velocity subsonic flows and and accelerating inwards to supersonic speeds. These processes take place on the two branches of the saddle singularity. The latter possibility also existed for the flows of figure 16.

At the extreme lower value of $\gamma = 1$, we have the situation shown in figure 20. At $\gamma = 1$, the gas has unlimited internal energy storage (the number of degrees of internal freedom is ∞) and this serves to maintain the temperature at a constant value. In this limiting case it is necessary to redefine our dimensionless variables. The equation for the curves of figure 20 has now become $W - \frac{1}{R} + \log \lambda / W R^4$.

Because of the great internal energy storage, the upper limit of the free particle flows, which has characterized previous graphs, has now disappeared. Also, since the internal energy is infinite, the distinction between positive and negative energy cases has disappeared. The saddle

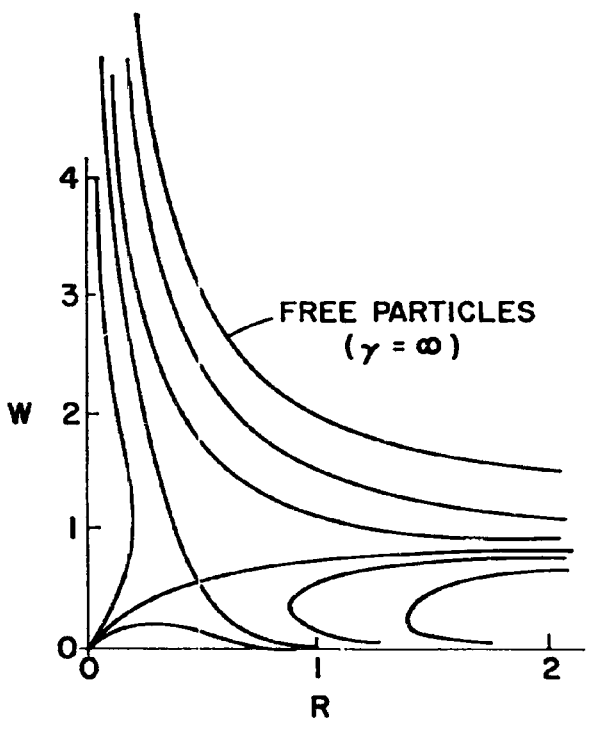

Typical Curves for $1 < \gamma < 3/2$
Positive Energies

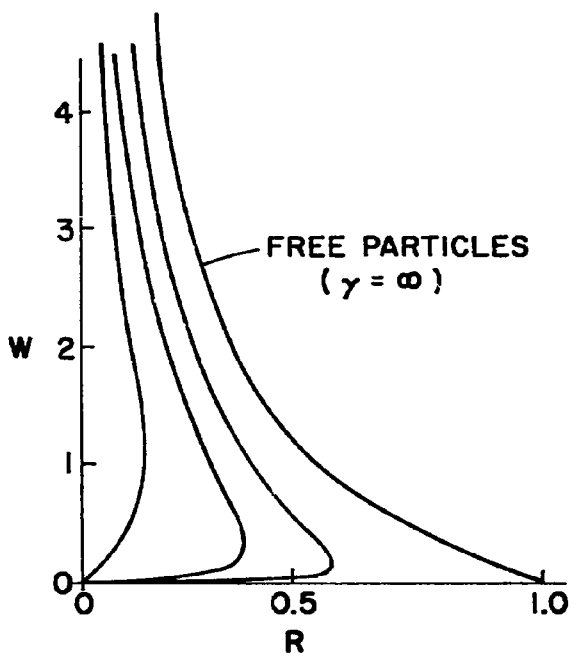

Typical Curves for $1 < \gamma < 3/2$
Negative Energies

Figure 19

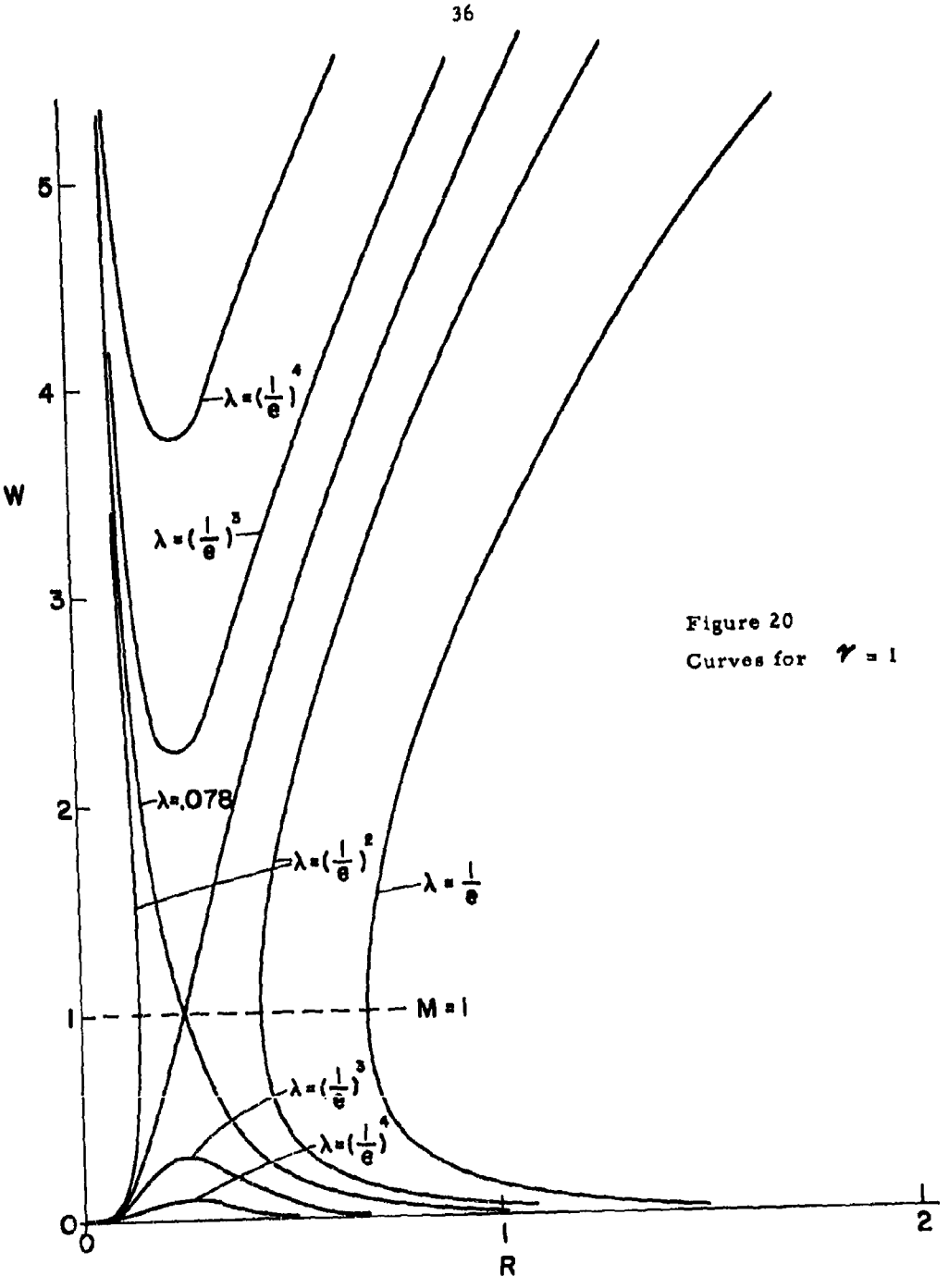

Figure 20
Curves for $\gamma = 1$

singularity is still present, offering the possibility of real transitions from subsonic to supersonic speeds. Now, however, the all-supersonic flows exhibit a minimum in their velocity curves corresponding to the maximum in the velocity curves of the all subsonic flows which appeared earlier. These maxima and minima now all occur at the same dimensionless radius.

Flows Into and Away From Stars

At this point, let us turn our attention to applying the results of these curves to the problem of flow into and away from stars. As mentioned earlier, we propose to attack this problem in the following way. The star itself is tending to boil away its atmosphere or corona. Conditions at the outer edge of the atmosphere or corona will thus impose one set of restrictions on the flow field. The interstellar medium, containing gas at a finite density temperature and pressure, will impose another set of conditions on the flow field.

We can immediately make two far-reaching statements. First---none of the negative energy flows can correspond to reality for stellar flow fields. The reason is that none of the negative energy flows have a finite pressure at $R = \infty$ to balance the corresponding pressure of the interstellar medium. Second---for positive energy flows, we may not end up with supersonic flows at $R = \infty$. These, too, all have zero pressure and thus can not balance the pressure of the interstellar medium.

The only circumstance that would permit us to use negative energy cases, would be that all stars had negative energy atmospheres and thus managed to hold their atmospheres without flow by means of the gravitational field. In this case the interstellar medium could be a void. However, as soon as some stars pour forth material into the interstellar medium and thus give it a finite pressure, we must use positive energy cases for all stars.

Let us begin our analysis by examining flows that move inwardly toward the star. We assume that the interstellar medium acts as a

reservoir capable of supplying an unlimited amount of gas at a fixed pressure and temperature. We consider a fixed surface surrounding the star and ask what happens as we vary the "back pressure" at this surface.

If p_∞ and c_∞ are the pressure and the velocity of sound in the interstellar medium and if p_s and V_E are the pressure and escape velocity at the fixed surface surrounding the star, then the back pressure corresponding to no flow, in or out, is given by

$$p_{s_{\text{NO FLOW}}} = p_\infty \left[1 + \frac{\gamma-1}{2} \cdot \frac{V_E^2}{c_\infty^2} \right]^{\gamma/\gamma-1}$$

If we lower p_s below this value, there will be an inward flow of gas. When p_s reaches the value

$$p_{s_{\text{Sonic}}} = p_\infty \left(\frac{2}{\gamma+1} \right)^{\frac{\gamma-1}{\gamma+1}} \left[1 + \frac{\gamma-1}{2} \cdot \frac{V_E^2}{c_\infty^2} \right]^{\gamma/\gamma-1}$$

the flow will be sonic at the surface. If we now turn to figures 12 to 19, we readily verify that the dimensionless parameters $\bar{W}$ and R are given by $\bar{W} = \frac{\gamma-1}{2} \frac{u^2}{c_\infty^2}$ $\qquad R = \frac{2}{\gamma-1} \cdot \frac{c_\infty^2}{V_E^2} \cdot \frac{r}{r_s}$

Since c_∞ is about 3/4 km/sec and since V_E for stars is 100's of km/sec, it is clear that when $r = r_s$, R will be very small compared to unity. Hence our fixed surface will correspond to values of R very near the origin of figures 12 to 19.

If we examine figures 12 to 19 carefully we see that only when γ if equal to or greater than 5/3 does a real set of solutions exist from R = ∞ to very small values of R for the full range of p_s between $p_{s_{\text{no flow}}}$ and $p_{s_{\text{sonic}}}$, i.e. between the solution $\bar{W} = 0$ and the solution having M = 1 at $r = r_s$. For such values of γ, the flow with $p_s = p_{s_{\text{sonic}}}$ steadily accelerates as it moves inward and, by the time it has reached r_s, its large gravitational energy has been converted into

comparable proportions of kinetic and thermal energy. Both of these energies will be large compared to the thermal energy of the interstellar medium, i.e. W_S will be large.

Now we must determine what happens to flows having γ less than 5/3 when p_s varies between $p_{s\,\text{no flow}}$ and $p_{s\,\text{sonic}}$. In these cases, there is a value of p_s relatively close to $p_{s\,\text{no flow}}$, for which the flow will reach sonic speed at an intermediate R (less than, but not greatly different from unity) and will subsequently experience a decrease in Mach number as it proceeds inward to R_s. (For γ's between 3/2 and 5/3, the velocity will continue to rise even though the Mach number is falling.) Thus the flow has choked out in the field beyond the surface surrounding the star. If we now lower p_s below this choking value, we should expect, on the basis of our earlier experience with the flows of figure 1, that the flow will make a transition to supersonic speeds (through the saddle singularity) and then will experience a shock wave jump back to subsonic speeds before reaching r_S. The shock wave will steadily move toward r_S as p_s is lowered, until it moves past r_S, providing a sudden drop in the permissible values of p_s.

Now let us look more closely at conditions near the star itself. What is happening to the flow after it passes r_S? At r_S, the combined kinetic and thermal energies of the flow are comparable with the escape energies of the star, and since stellar surface temperatures usually correspond to much lower energies, it is clear that major dissipative energy transfer processes must take place near the star between the incoming flow and the star itself. Thus the incoming flow is rapidly cooled or "condensed". This process will resemble what is called a condensation shock. The flow will be rapidly decelerated to low speed, after which, the incoming gas will simply become a part of the star's atmosphere.

If we add this picture of a condensation shock to our preceding picture of an incoming flow, we see that the condensation can readily lower the pressure of p_s to values appropriate for incoming sonic flow.

If γ is less than 5/3, it may happen that the condensation is sufficiently strong so that the regular shock wave in the flow moves inward until it joins with the condensation shock.

If we were to examine the structure of the condensation shock more carefully, it is quite possible that we should see a situation not unlike the corona of the sun, i.e. a very hot gaseous envelope surrounding the star with a rather rapid transition to the surface temperatures of the star.

In summary, we find that when γ lies between ∞ and 5/3, the amount of the inflow depends upon conditions existing near the star. If

$$p_s = p_\infty \left[1 + \frac{\gamma-1}{2} \cdot \frac{V_E^2}{C_\infty^2}\right]^{\gamma/\gamma-1}$$

, there is no inward flow

If $p_s = p_\infty \left(\frac{\gamma-1}{\gamma+1}\right)^{\frac{\gamma-1}{\gamma}} \left[1 + \frac{\gamma-1}{2} \cdot \frac{V_E^2}{C_\infty^2}\right]^{\frac{\gamma}{\gamma-1}}$ the inward flow reaches sonic velocity at S and the total mass flux is given by

$$16\pi \rho_\infty \frac{G_1^2 M^2}{C_\infty^3} \left(\frac{C_\infty}{V_E}\right)^4 \left[\frac{2}{\gamma+1} + \frac{\gamma-1}{\gamma+1} \cdot \frac{V_E^2}{C_\infty^2}\right]^{\frac{1}{2} \cdot \frac{\gamma+1}{\gamma-1}}$$

. It is suggested that condensation near the star determines the pressure level and if this is so, it is likely that for most stars the condensation is sufficiently rapid to maintain the flow at this latter value. For flows with γ between 1 and 5/3, there will be a relatively narrow band of pressure, p_s, just below the value $p_\infty \left[1 + \frac{\gamma-1}{2} \frac{V_E^2}{C_\infty^2}\right]^{\gamma/\gamma-1}$ in which conditions near the star can affect the amount of the flow. For pressures below this band, the flow will choke at relatively great distances from the star and then the flow will be "frozen" at the value

$$\frac{\pi}{4} \cdot \rho_\infty \frac{G_1^2 M^2}{C_\infty^3} (5-3\gamma)^2 \left[\frac{2}{\gamma+1} + \frac{\gamma-1}{\gamma+1} \cdot \frac{V_E^2}{C_\infty^2}\right]^{\frac{1}{2} \cdot \frac{\gamma+1}{\gamma-1}}$$

regardless of conditions at the star. Again, the condensation is likely to be sufficiently strong to cause this choking to take place.

At this point, let us turn our attention to the question of outward flows from stars. Here we ask the corona to play a more dominant and active role. We accept the fact the corona is non-isentropic and attempt to fit our flow patterns to the outer boundaries of the corona, hoping that beyond some such boundary the flow will be able to be described by polytropic processes.

We attack this problem in the following way. We hold conditions constant at the outer coronal surface and examine what happens to the flow as we vary the pressure in the interstellar medium.

When the pressure in the interstellar medium is zero, the gravitational field will prevent any flow from occurring until the energy of the gas becomes positive. This can be restated in the following way. The corona will be unable to expel material until it reaches a "boiling" temperature such that the velocity of sound in the gas, $C_s = \sqrt{\gamma R T_s}$, at the outer coronal surface exceeds $\sqrt{\frac{\gamma-1}{2}} \cdot V_E$, where V_E is the escape velocity at this surface.

Let us assume that this condition is satisfied. We then find that if the pressure of the interstellar medium has the value

$$p_{\infty\ \text{No Flow}} = p_s \left[1 - \frac{\gamma-1}{2} \cdot \frac{V_E^2}{C_s^2} \right]^{\frac{\gamma}{\gamma-1}},$$ no flow will take place, because the interstellar medium will exert sufficient back pressure to stop the flow. As we lower p_∞ below this value, outward flow will occur and when p_∞ reaches the value,

$$p_{\infty\ \text{Choke}} = p_s \left[\frac{\gamma+1}{2} - \frac{\gamma-1}{2} \frac{V_E^2}{C_s^2} \right]^{\frac{\gamma}{\gamma-1}}$$ this flow will attain sonic velocity at the outer coronal surface. In order to see what is happening at intermediate radii, let us refer to the results of

figures 12 to 20. First we must determine the appropriate scale factors for the dimensionless variables W and R. We find that

$$W = \frac{u^2}{\frac{\gamma+1}{\gamma-1} c_s^2 - V_E^2} \qquad \text{and} \qquad R = \frac{r}{r_s}\left(\frac{\gamma+1}{\gamma-1}\cdot\frac{c_s^2}{V_E^2} - 1\right)$$

Since we agreed earlier to assume that c_s^2 is greater than $\frac{\gamma-1}{2} V_E^2$ we see that both W and R will be positive, as they should be. At the outer coronal surface, $r = r_s$ and $R_s = \frac{\gamma+1}{\gamma-1}\cdot\frac{c_s^2}{V_E^2} - 1$.

Now we must distinguish between the different ranges of γ. When γ is less than 5/3, a sonic throat can occur in the flow as indicated by the appearance of a saddle singularity. In figures 16, 17 and 19, this saddle singularity occurs at $R_c = \frac{5-3\gamma}{4(\gamma-1)}$. This sonic throat will be located outside the coronal surface if c_s is less than $V_E/2$. However since we must also have γ less than 5/3 and c_s greater than $\sqrt{\frac{\gamma-1}{2}}\cdot V_E$ for this exterior choking condition to exist, we see that it can in fact occur only when γ is less than 3/2. Thus we conclude that if $1 < \gamma < 3/2$ and $\sqrt{\frac{\gamma-1}{2}} < \frac{c_s}{V_E} < \frac{1}{2}$, then, as we lower the pressure, p_∞, below $p_s\left[1 - \frac{\gamma-1}{2}\cdot\frac{V_E^2}{c_s^2}\right]^{\gamma/\gamma-1}$ the flow will reach sonic velocity and choke at some radius exterior to the coronal surface before it is limited by sonic velocity at the coronal surface.

What happens when the pressure, p_∞, is lowered below this exterior choking value? There is then no continuous curve linking up conditions at the coronal surface with conditions in the interstellar medium. Here, our earlier experience with the configuration of figure 1 comes to our assistance. We see that the flow emanating from the coronal surface will pass through sonic velocity at some external radius, and after becoming supersonic, will experience a shock wave, which will abruptly decelerate it to subsonic speeds. The flow will then continue out to great radii at

subsonic speeds. (As long as there is a finite pressure in the interstellar medium, the flow can not continue outwards at supersonic speeds, because all supersonic flows end up with zero pressure at $R = \infty$.) The shock wave will first appear just downstream of the sonic point, and as p_∞ is lowered, the shock wave will progressively move outward. Since it is unlikely that processes can occur in the gas which will cause γ to be close to unity at great distances from the star and since the exterior choking radius can never be large compared to the coronal radius unless γ is near unity, we see that when external choking does occur, it will always occur relatively close to the coronal surface.

When γ is greater than 3/2 or when C_s is greater than $V_E/2$, then sonic velocity will first occur at the coronal surface and the entire external flow will be subsonic. Under these circumstances, what occurs when we lower p_∞ even more? We should expect the sonic flow emanating from the coronal surface to choose the upper limb of the hairpin curve and accelerate to supersonic speeds. It will then experience a shock wave and continue outwards at subsonic speeds. The shock wave will first appear just outside the coronal surface and will move progressively outwards as p_∞ is lowered.

The above explanation has the following difficulty. We are, in reality, asking the continuous transition from subsonic to supersonic flow to take place at the outer limit of the non-isentropic corona. We do so for cases where such a transition is not possible in isentropic flow. Since we are closing our eyes to what is happening in the corona, are we not now asking fluid dynamic as well as thermodynamic magic to occur in the corona? Strictly, we can not answer this question without attacking the corona problem itself. However, in so far as coronal processes can be treated as polytropic processes with fictitious isentropic exponents, we should expect γ to be near unity (or even below unity). If we accept this view, then the coronal flow is represented locally by a family of curves from our figure 20. And from such curves we can obtain a real transition

from subsonic to supersonic speeds within the corona. E. H. Parker has, in fact, used just such an isothermal flow with a transition from subsonic to supersonic speeds to fit the observed data for the solar corona and has obtained satisfying agreement.

In summary, we see that for outward flows to take place, it is necessary that the coronal surface temperature T_s be greater than $(\gamma-1) V_E^2/2\gamma$. Furthermore, the pressure in the interstellar medium must be less than $p_s \left[1 - \frac{\gamma-1}{2} \cdot \frac{V_E^2}{C_s^2}\right]^{\gamma/\gamma-1}$

For lower values of p_∞, an all-subsonic outward flow will first make its appearance. If γ is less than 3/2 and C_s/V_E lies between $\sqrt{\frac{\gamma-1}{2}}$ and $\frac{1}{2}$, sonic velocity will first appear in the flow at radii beyond the coronal surface. Otherwise, ~~some~~ sonic velocity will first appear at the coronal surface. For still lower values of p_∞, supersonic velocities will appear beyond the sonic point, followed by a shock wave which converts the flow back to subsonic speeds. When the sonic velocity occurs at the coronal surface, the total outward mass flow is simply $4\pi \rho_s c_s r_s^2$. When the sonic velocity occurs beyond the coronal surface, the outward flow is somewhat less than this amount.

It is interesting to note that in considering both inward and outward flows we have arrived at quite different criteria for the condition of no flow. The reason for this is, of course, that in one case we have assumed the entire field to have the thermodynamic constants of integration appropriate to the outer boundary conditions and in the other case appropriate to the inner boundary conditions. There is no reason why, for individual stars, these should agree. It is quite possible that our criteria could predict the simultaneous possibility of an inward and an outward flow or the simultaneous impossibility of both. In the latter contingency, it is always possible to patch together two stationary fields, the inner one consisting of gas from the inner boundary and the outer one of gas from the outer boundary, to satisfy conditions appropriate for a stable static field.

In the former contingency, any such patched field is unstable and one or the other of the gas masses will expel the other and establish its own steady flow.

If the gas in the interstellar medium has emanated from the stars, then, its thermodynamic constants should agree with some appropriate average value of the thermodynamic constants of the stars. In this case, it would not be surprising if a statistical study showed some agreement between the two criteria.

UNCLASSIFIED